Results in Engineering 21 (2024) 101827

Contents lists available at ScienceDirect

Results in Engineering

journal homepage: www.sciencedirect.com/journal/results-in-engineering

The question of thermoelectric devices (TEDs) in/efficiency—a practical examination considering thermoelectric coolers (TECs)

Nganyang Paul Bayendang *, Vipin Balyan, Mohamed Tariq Kahn

Cape Peninsula University of Technology, Department of Electrical, Electronic and Computer Engineering, Bellville Campus 7535, Cape Town, South Africa

ARTICLE INFO

Original content: Supplementary Material (Original data)

Keywords:
Thermoelectrics (TE)
Thermoelectric devices (TEDs)
Thermoelectric coolers (TECs)
TE modules (TEMs)
Thermoelectric cooling system
TECs in/efficiency
Thermoelectricity in/efficiency

ABSTRACT

Thermoelectric devices (TEDs) are clean energy devices with diverse applications; however, the question of their energy in/efficiency and how to improve it, has been a subject of research/debate among many researchers and non/users. In an effort to contribute to this quest/scientific discourse, this paper focuses on energy in/efficiency in TEDs when operated as thermoelectric coolers (TECs) for cooling purposes. A practical research was performed using sixteen identical TECs operated in the same performance test conditions and powered in turns using 12 V, 10 V, 8 V, 6 V and 4 V, with a 5 A current limit, to investigate TECs in/efficiency inconsistency. It was found that the TECs (TEC-12706 from the same manufacturer) used in the study all performed differently under identical test setup; however, they all performed optimally at 8 V, with the best (TEC3) attaining a cooling of −4.81 °C with an input power of 21.09 W and the worst (TEC9) attaining a cooling of 12.63 °C with a power input of 45.52 W. From our findings, TECs in/efficiency can therefore be summarily attributed to five fundamental factors and though TECs efficiency is well known to be limited by 1) its intrinsic p-n junction semiconductor chemistry and physics at materials level; however, we can conclude that given the same semiconductor technology, TEC inefficiency is further exacerbated by 2) low-quality manufacturing/assembly at module level, 3) inadequate designs at application/system level, 4) substandard system construction/workmanship at implementation level and 5) general lack of theoretical/physical knowledge of TECs operation at users' level.

1. Introduction

Energy sustainability over the past decades as defined in national and international governmental and non-governmental policies [1], has been at the centre of research in academia, research institutes and industries. Addressing energy insecurity is not mostly about focusing on alternative energy sources but also on the load, as that's where the energy is ultimately used. Therefore, the more energy efficient a load is, the less energy it consumes and the more energy will be available for others. Cooling is a fundamental necessity in most households and businesses [2], as it lends itself to various applications which include but not limited to refrigeration, air-conditioning and general cooling applications. Cooling can be produced in various ways which include but not limited to the use of chillers, laser and thermoelectricity using a thermoelectric cooler (TEC) based on the Peltier effect—production of cold or heat when a direct current (DC) flow creates a temperature difference at the junctions of two different semiconductor materials [3]. This paper focuses on i) producing cooling using TECs and ii) to study different aspects of cooling and energy in/efficiency when the same kind of TECs are used in an identical test setup and operating conditions. In light of this, a wide variety of literature on TEC in/efficiency are reviewed in what follows to set the basis on which our research is founded and conducted.

According to Ref. [4], TEC has also found itself useful in performing cooling in clothing. They conducted a study to determine the influence of heatsinks and to select the best operating mode of the controller and the TEC modules position/arrangement on the body by comparing the different cooling efficiency. Similarly, in Ref. [5], their work focused on the cooling and energy efficiencies, as well as power consumption aspects of personal cooling system based on flexible TECs using a single participant. The preliminary results for the determination of energetic efficiency of thermoelectric cooling system using a numerical method was presented in Ref. [6]. The results of their numerical calculations showed the influence of power supply current on the efficiency of cooling characteristics, as well as air temperature distribution inside their experimental room. A theoretical examination on the effect of

* Corresponding author.
E-mail address: bayendangn@cput.ac.za (N.P. Bayendang).

https://doi.org/10.1016/j.rineng.2024.101827
Received 1 November 2023; Received in revised form 17 December 2023; Accepted 22 January 2024
Available online 1 February 2024

input power, velocity of inlet working fluid, the arrangement of the TEC modules used and the type of fluid on the thermoelectric cooling system performance including the coefficient of performance (CoP) and the rate of heat transfer, were provided in Ref. [7]. Articulated in Ref. [8] is a summary of energy balance model parameters representing different performance aspects of building-integrated thermoelectric cooling-photovoltaic (TEC-PV) devices. Understanding the relationship between TEC materials electrical and heat conductivities is essential to improve the CoP efficiency [9]. TEC efficiency depends on the figure of merit, which is depended on the best TEC material used. Their TECs review crucial finding informs that, the higher the electrical conductivity and the lower the thermal conductivity, the higher is a TEC's CoP. High power electronic devices require cooling and TECs with heatsinks are mostly used. Maximizing TECs cooling power was studied in Ref. [10] and the effect with respect to variations in the thermoelectric (TE) geometry was discussed—in which they asserted that among various factors, TECs cooling power can be dramatically enhanced at low leg lengths and with a better heatsink material. By employing a density-based topology optimization approach by spatially distributing two different thermoelectric materials in a two dimensional design space, [11] demonstrated that TECs efficiency and cooling power can be respectively enhanced by 11.4 % and 48.7 % relative to other optimization results in the literature. The concept of annular thermoelectric cooler (ATEC) was introduced in Ref. [12], whereby an ATEC exo-reversible thermodynamic model considering the Thomson effect in conjunction with the Peltier effect, Joule heating and Fourier heat conduction, were investigated using exergy analysis. Their findings revealed that the Thomson effect increases ATEC cooling power and energy/exergy efficiencies, though lower than those of conventional flat plate TECs. Notwithstanding, ATEC will be more helpful and preferable in applications which requires cooling of fluid flowing through pipes and cooling of cylindrical structures. Theoretically studied in Ref. [13] are the heatsink geometry, fin number, fin length and dimensions to examine a TEC performance under three variables of power, airspeed and ambient temperature. Heatsink was used on the hot and cold sides. The results showed that the cooling capacity increased with increase in airspeed and the maximum cooling capacity was 180 W at an airspeed of 4 m/s and TEC power of 300 W. In Ref. [14], presented is a brief theoretical guide on how to select a TEC, in which various design considerations were highlighted, including minimizing or eliminating the effects of condensation on the TEC and neighbouring parts when designing with TECs in sub-ambient cooling applications. Designing with TECs can be a cumbersome exercise due to the various manufacturers having proprietary info with datasheet that have technical discrepancies; as a result, presented in Ref. [15] was a new operational framework for an internet based thermoelectric cooling system design process that would facilitate the interaction and collaboration between TEC designers and manufacturers. The main problem over the use of TEC is the limited CoP and its thermal performance—researched in Ref. [16] was the use of multistage TEC to enhance both. TEC geometrical dimension and shape have vital impact on its cooling performance and thermal-mechanic characteristics, which according to Ref. [17] were hardly investigated in previous TEC research. To bridge this gap, their work reported the development and operation of a novel three-dimensional model for TECs with 10 different leg geometries.

The cooling capacity (Qc) and CoP are both important performance parameters of a TEC. Simulated in Ref. [18] are three-dimensional numerical finite element analysis based on TEC temperature-dependent materials properties. It was found that electrical current, geometric configuration of thermoelectric element leg, the Thomson effect, thermal and electrical contact resistances affect TEC performance. They performed a multi-objective optimization using genetic algorithms based on TOPSIS (technique for order preference by similarity to an ideal solution) and NSGA-II (non-dominated sorting genetic algorithm). A trapezoid-type two-stage Peltier couples (TTPC) for use in two-stage thermoelectric cooling applications was presented in Ref. [19]. By employing the TTPC units without intermediate ceramic plates, the TTPC based thermoelectric module may reduce the inter-stage thermal resistance that could provide optimal CoP and Qc. Stress is a vital aspect when designing with thermoelectric (TE) devices. Investigated in Ref. [20] is a TEC thermo-mechanical analysis. They examined the influences of electrical current, leg length, ceramic plate and bonding layers on the thermal stress level. It was found that the thermal load attached to the Peltier junction can cause extreme high levels of thermal stress, which might cause dislocations and cracks of the material layers. They presented an optimized design with predictive thermo-mechanical performance to achieve minimum thermal stress levels, which provided a useful guide to realise high reliability in a compact TEC. Using TECs efficiently requires proper understanding of the factors that influence its performance and efficiency during the installation design phase. As a result, [21] reviewed various TEC studies and attested that the Joule heating effect, temperature difference across the TECs and thermal conductance between the p-n junctions, influence TECs CoP and efficiency. The thermal performance of thermoelectric air-cooling module consisting of a TEC and an air-cooling heatsink was examined in Ref. [22]. The influences of input current and heat load were determined and they showed that TECs are more effective under low heat loads and at a supply current of about 6 A. Increasing the input current decreases the TEC electrical resistance while it increases the heatsink resistance. Contrarily, an increasing heat load increases the TEC electrical resistance while it decreases the heatsink resistance. Investigated in Ref. [23] is the performance of a one-stage TEC using mathematical and thermodynamic modeling. A new correlation for performance evaluation of a TEC combined with two heatsinks was proposed. It was found that the maximum cooling power of their system takes place at 14 V, which was the system optimum voltage. Furthermore, decreasing the thermal resistance of the TEC hot-side heatsink raised the cooling power and on the contrary, increasing the thermal resistance of the TEC cold-side heatsink decreased the system cooling power. A review on PV-powered TEC was conducted in Ref. [24] and it was opined that the cooling performance of a segmented thermoelectric element is superior to that of traditional TECs. They further stated that there are two main strategies to attain performance enhancement of TECs, which are; enhancing the inherent efficiency of the thermoelectric materials (the dimensionless figure-of-merit zT, should be > 0.7) used and by improving the thermal design of TECs by enhancing the contact resistance, thermal interfaces and heatsinks. Power management is paramount to enhance energy efficiency. Proposed in Ref. [25] is an improved proportional integral differential (PID) algorithm with energy feedback based-on state machine and H-bridge, employed to control in real-time TE cooling by alternatively charging and discharging two groups of batteries efficiently. TE devices cooling and heating dual feature makes it ideal as a solid state refrigeration and heat-pump system. Investigated in Ref. [26] is a battery thermal management system (BTMS) for electric vehicles (EV) and hybrid electric vehicles (HEV) to manage heat generation during operation of the battery pack, in which heat produced by the battery pack is transported to the TEC cold side and then released by the heatsink to the surrounding. Their system gave different cooling results when tested using different power supply voltages. While TEC number of modules, input power and thermal fluids are well known to affect TECs CoP, exergetic efficiency and cost per unit of cooling; the extent to which each affects was studied in Ref. [27] by employing the Taguchi method—whereby the number of TEC modules, power input and airflow rate are varied in turns. Their findings revealed that TEC number of modules has the most effect followed by the power input and then air flow. A similar study was performed in Ref. [28]. Nowadays, solar energy is the most explored and common source of renewable energy. Nonetheless, according to Ref. [29], photovoltaic (PV) cells get very hot which affects their efficiency. Their research involved integration of TEDs to cool the PV panels and also to convert the heat energy to power, thereby increasing the solar cells efficiency by 15 %. Air conditioning is used in various settings, one of which being in a locomotive. In Ref. [30], a TEC with 199 thermoelectric elements having a 450 W maximum cooling capacity was initially devised, afterwhich 16 of these TECs were employed to design a kilowatt scale thermoelectric air conditioner (TEAC) system to provide noise free air-conditioning in a high-speed train driver cabin. Their TEAC achieved a 2.342 kW cooling capacity with a CoPc of 0.5 in cooling mode and a 3.5 kW heating capacity with a CoPh of 1.3 in heating mode.

From the diverse past literature examined, TECs find itself in various applications and it's clear there are many factors that affect TECs efficiency and at various levels – from the semiconductor chemistry choice, via the physics, as well as engineering and to the end users' utilization. While TECs in particular and thermoelectricity in general performance is limited by the semiconductor materials figure of merit (z) and there is very little that can be done to improve the performance once a particular semiconductor chemistry is chosen during manufacturing; however, the TEC module figure of merit (Z) is affected by several physical aspects and a lot can be done to improve the performance during and after manufacturing, failure of which will make the TEC performance and efficiency degrade further from bad to worst. This research article is set to fill in the gap identified—which is i) to study cooling and energy in/efficiency of the same kind of TECs employed in identical tests setup and ii) to demystify the generalized TECs' poor performance stigma; notably experience at the design, implementation and users' levels.

This manuscript is structured as follows: A succinct background of TECs literature with focus on inefficiency was introduced in Section 1, followed by presentation of the research materials and methodology employed in Section 2. Asserted thereafter is the research results in Section 3. The results are elaborately analysed in Section 4. Lastly, the closing comments with recommendations for further studies are articulated in Section 5.

2. Research materials, methods and methodology

The various materials, methods and methodology utilised to conduct the research are explained in what follows.

2.1. Materials

The following materials (herein don't refer to TECs semiconductor but mean devices, components, equipment, sensors and other vital items) were used in the study.

- x16 TEDs operated as TECs (model # TEC-12706; NB: all are the same type)
- x32 aluminium heatsinks (L6 x W4 x H2.5 cm)
- x4 Sinilink XYS3580 (0.6–36V/5A) DC-DC buck-boost converters
- x2 12 V/18 A Power Man PC power adapter (model #: IP-S300FF7-0 H)
- 9–24 V/5 A AC-DC power adapter (model #: Huazhenyuan-009)
- x3 MAX6675 temperature sensors
- x16 DS18B20 temperature sensors
- DS18B20 temperature sensors breakout board
- Keyes ESP32 Wroom-32 development board
- Arduino IDE version 1.8.19
- x3 Geekcreit MOSFET driver boards
- x2 12 V DC water pumps
- x2 12 V electric solenoid valve
- Fluke Ti20 thermal imager
- Toptronic T235H multimeter
- A K-type thermocouple
- x2 bathtubs (L36 × W26 × H12 cm)
- A metal tray (L35 × W26 × H4cm)
- A drip tray (L75 × W44 × H4cm)
- Water pipes
- Thermal paste (heatsink compound)
- High temperature glue
- Fasteners (screws, nuts, washers, Prestik putty etc)

2.2. Methods

This simply shows/explains how the miscellaneous materials listed in Section 2.1, were set up together and applied to execute the research.

2.2.1. TECs-heatsinks assembly

This demonstrates how the TECs were set up and assembled with the heatsinks. A total of 16 TECs were used for the experiment. The TECs were each uniquely identified and arranged as exemplified in Fig. 1. As shown in Fig. 2, the metal tray was cut into 16 square holes corresponding to the dimension of each TEC module. Two holes were drilled on each square hole sides in the metal tray. Each TEC was carefully inserted in a square hole in the metal tray with the TEC cold side facing up. The TECs were glued in place to prevent water leaks between the bottom and top sections. Heatsink paste was uniformly applied first on each TEC hot side. Each TEC bottom heatsink was mounted and the screws and washers put in place to secure the bottom heatsink on each TEC hot side. Thereafter, heatsink paste was uniformly applied on each TEC cold side. Each TEC top heatsink was mounted, followed by adding the washers and nuts to secure each top heatsink on each TEC cold side. Prestik putty was then put on each nut to prevent rust.

2.2.2. Temperature sensors/instruments employed

This section discusses the various temperature devices used in the study. The Fluke Ti20 thermal imager was used to capture cold maps of the TECs cold side when conducting the different experiments. The K-type thermocouple was used with the Toptronic T235H multimeter to measure and note the ambient temperature in the lab when conducting the different experiments the TECs were subjected to. Placing the TECs sensors was very crucial. Three MAX6675 temperature sensors were used to measure the TECs hot side temperature by dipping their K-type thermocouples probe in different sections of the water used to cool the TECs hot side. Due to design difficulties, these thermocouples probe were not placed exactly on the TECs hot side heatsink but rather inside the water cooling the TECs hot side heatsink. However, knowing the TECs hot side exact temperature wasn't really crucial for the experiments. Three temperature sensors were used for the TECs hot side temperature measurements to ensure the right temperature readings were recorded. The average TECs hot side temperature was then used in the computations where necessary. Measuring the TECs cold side temperature was of most importance; as a result, each temperature sensor probe was placed inside each TEC cold side heatsink grove to ensure the probes were closest to the heatsink surface in contact with the TEC cold side. The MAX6675 temperature sensor doesn't measure below 0 °C; however, it variant MAX31855 can measure up to −200 °C but it's quiet expensive and most vitally, it's based on the SPI interface akin the MAX6675. Consequently, it becomes very impractical and expensive considering 16 TECs cold side temperature measurements were to be taken. The DS18B20 was the suitable alternative considered, as i) it can measure up to −55 °C (just within the TEC limit), ii) it is based on the One-wire interface requiring just one microcontroller pin and power lines for all 16 of them and iii) so affordable ($1/pc). Fig. 3 shows the temperature devices discussed.

2.2.3. Electronic boards employed

Four board types were used to interconnect different parts of the setup to each other. The boards include the ESP32 development board, the MOSFET driver boards (x2), the DS18B20 breakout board (which interfaced all the sixteen DS18B20 temperature sensors) and the MAX6675 boards (x3). The ESP32 development board (with Wroom-32 chipset) is the main board used to control all aspects of the experiments. A code was written with the Arduino IDE to read and process temperature measurements from the three MAX6675 and the sixteen DS18B20 temperature sensors, as well as to control the pumps through the

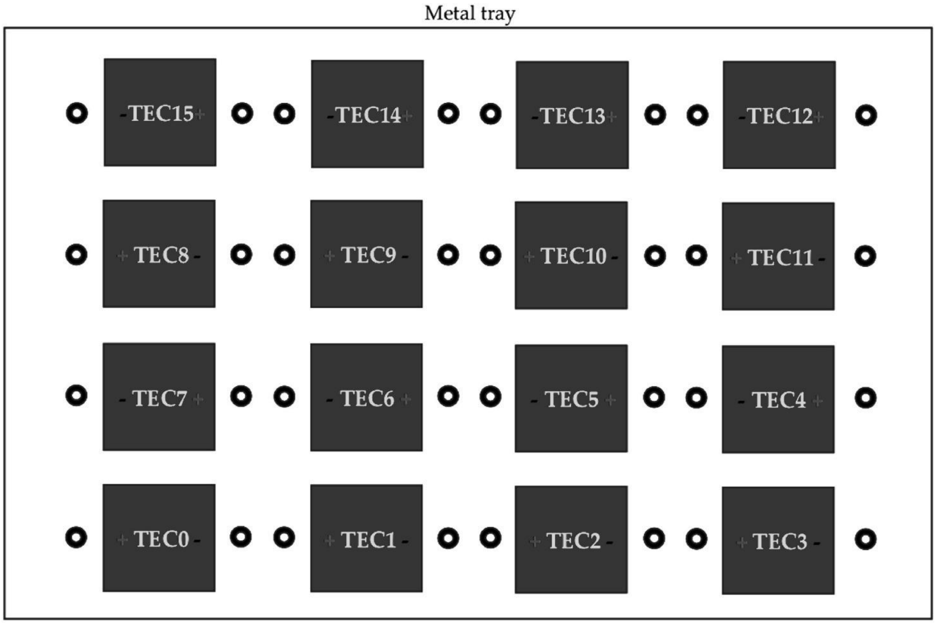

Fig. 1. Arrangement of the 16 TECs in the metal tray (top view showing TECs cold side).

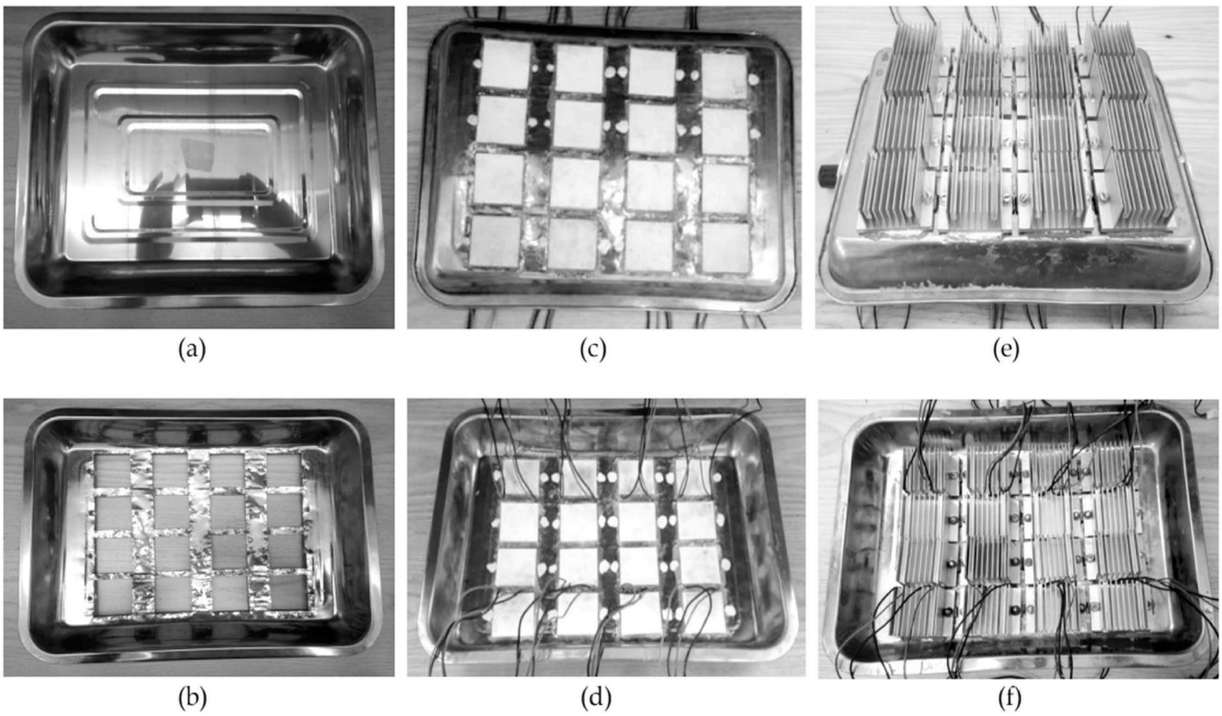

Fig. 2. Assembly of the 16 TECs in the metal tray (a) the metal tray, (b) the metal tray cut into 16 square holes, (c) bottom view of the 16 TECs inserted and glued in their respective square holes, (d) top view of the 16 TECs inserted and glued in their respective square holes, (e) bottom view of the 16 TECs with heatsinks and (f) top view of the 16 TECs with heatsinks.

MOSFET driver boards. Fig. 4 illustrates the boards employed.

2.2.4. Power supplies employed

Three different power supply types were used to power different parts of the setup. Two Power Man 12 V/18 A computer AC-DC power adapters (model #: IP-S300FF7-0 H) were used to supply the 16 TECs through four Sinilink XYS3580 (0.6–36 V/5 A) DC-DC buck-boost converters. Though one should suffice, to ensure enough power availability/capability, two Power Man PC AC-DC power adapters were used—each could supply 12 V x2/18 A x2, making a total of 12 V x4/18 A x4. However, because different voltages and current limit were needed to supply the TECs and in groups of four and in turns, a suitable DC-DC converter was needed, hence the incorporation of the four Sinilink XYS3580 (0.6–36 V/5 A) DC-DC buck-boost converters. To avoid overloading a power supply, it was setup such that two Sinilink power converters were supplied by a Power Man AC-DC power adapter. The Sinilink XYS3580 DC-DC converter is a nifty device with many vital features that include current, voltage and temperature limits and can

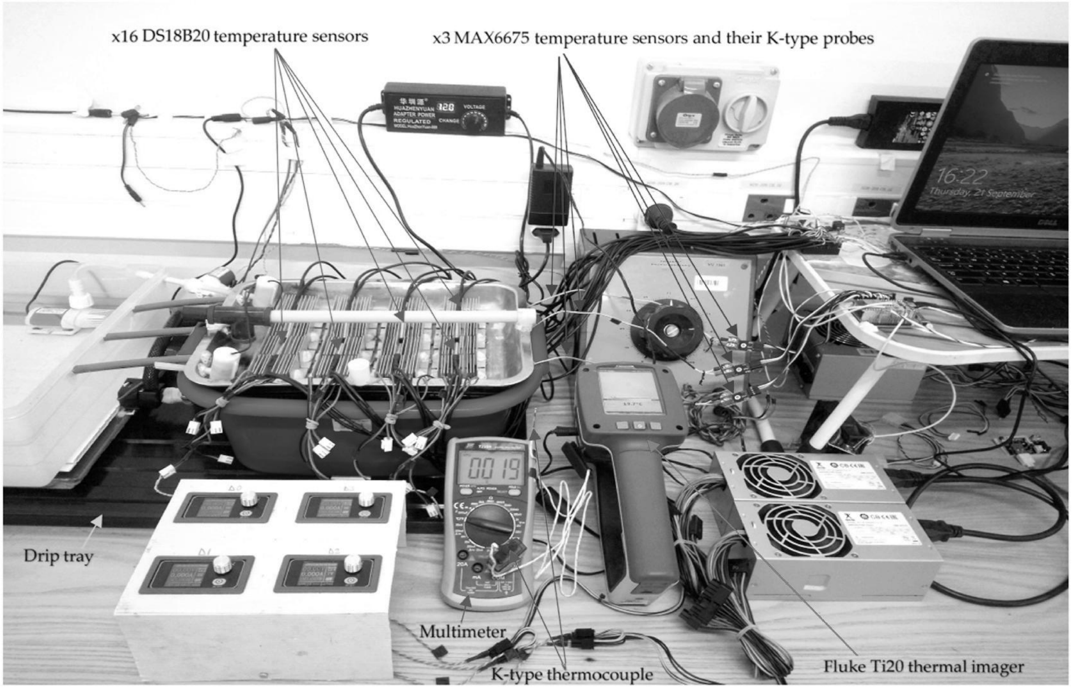

Fig. 3. Temperature sensors/instruments employed.

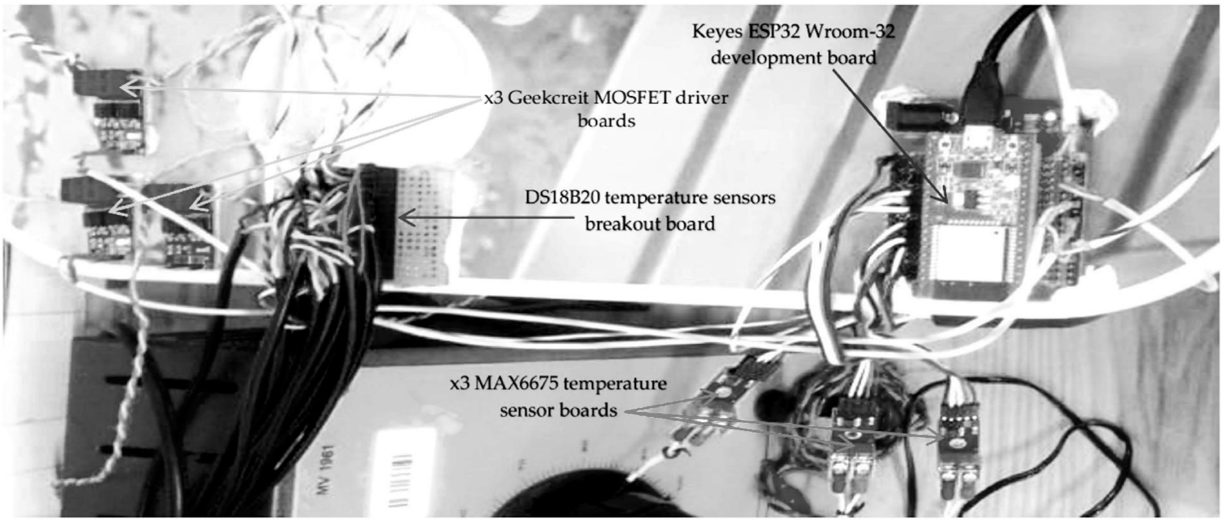

Fig. 4. Depiction of the different electronic boards used.

display the voltage, current, power, energy, capacity and graphs. The 16 TECs were arranged in 4 rows and 4 columns as depicted in Fig. 1 and each TEC row was tested in turns, whereby the four Sinilink power converter were each used to supply each TEC in a row—that is, one Sinilink power converter per TEC per row at a time. To protect the TECs, each Sinilink power converter current limit was set to 5 A and in turns set to 12 V, 10 V, 8 V, 6 V and 4 V as per the various experiments that were conducted. More on this later. The 9–24 V/5 A AC-DC power adapter (model #: HuazhenYuan-009) was used to power the x2 DC water pumps and the x2 solenoid valves. This power supply was set to 12 V and was controlled via pulse width modulation through the MOSFET driver boards connected to the ESP32 microcontroller board, to control the speed and switch ON/OFF the pumps as well as the solenoid valves. Fig. 5 shows the power supplies employed.

2.2.5. *Pumps and solenoid valves employed*

Two 12 V DC pumps and two 12 V DC solenoid valves were used to control the flow of water to the TECs hot side—which was submerged in a blue bathtub containing water. Each pump was connected to each solenoid electrically in parallel and hydrologically in series, giving two pump-solenoid valve pairs. Once the water in the blue bathtub temperature was above 22 °C, the power to the TECs will be switched OFF and the warm water pump-solenoid valve pair will pump the warm water out from the TECs hot side. Once emptied, the cold water pump-solenoid valve pair will pump cold water from the white bathtub to the blue bathtub housing the TECs hot side, to maintain its water temperature around 22 °C (± 3 °C) for the various experiments. Fig. 6 depicts the warm and cold water pumps-solenoid valves setup.

Fig. 5. Illustration of the power supplies used.

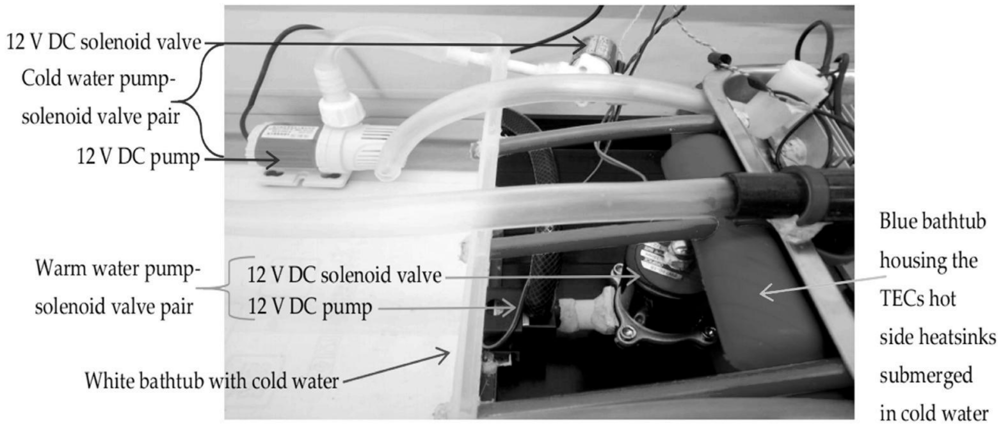

Fig. 6. Warm and cold water pumps-solenoid valves representation.

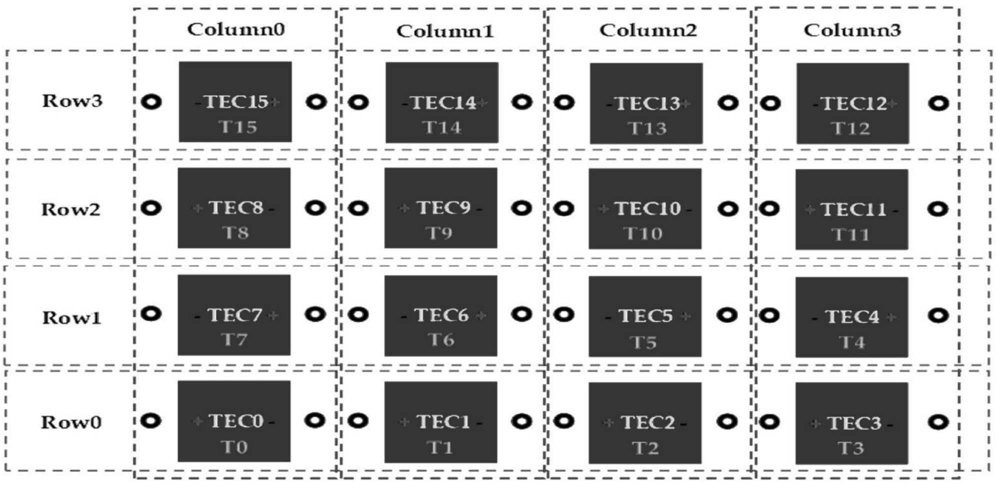

Fig. 7. TECs test matrix view from the cold side.

2.3. Methodology

This explains the workflow on how the various experiments were conducted based on the setup in Section 2.2. The 16 TECs were partitioned into 4 rows and 4 columns as shown in Fig. 7. Since only four Sinilink DC-DC power converters were used as displayed in Fig. 8, each TEC was tested one row at a time, starting from Row0 to Row3. That is, to test Row0; TEC0, TEC1, TEC2 and TEC3 were respectively connected to Sinilink DC-DC power converters, labeled D0, D1, D2 and D3. Once Row0 testing was done, Row1 was tested next by connecting TEC7, TEC6, TEC5 and TEC4 respectively to D0, D1, D2 and D3. To test Row2; TEC8, TEC9, TEC10 and TEC11 were respectively connected to D0, D1, D2 and D3 and finally to test Row3; TEC15, TEC14, TEC13 and TEC12 were respectively connected to D0, D1, D2 and D3. The idea is such that, whenever a TEC row is tested, a Sinilink DC-DC power converter a) D0; supplies power only to Column0 TECs (TEC0, TEC7, TEC8 and TEC15), b) D1; supplies power only to Column1 TECs (TEC1, TEC6, TEC9 and TEC14), c) D2; supplies power only to Column2 TECs (TEC2, TEC5, TEC10 and TEC13) and d) D3; supplies power only to Column3 TECs (TEC3, TEC4, TEC11 and TEC12). A total of 20 experiments were performed, whereby starting with Row0 TECs (TEC0 to TEC3); they were each supplied first with 12 V/5 A current limit, to measure the followings: i) the lab ambient temperature using the multimeter with the K-type thermocouple, ii) Row0 TECs hot side water temperature using the MAX6675 temperature sensors labeled TH0, TH1 and TH2 and the TECs hot side water average temperature (THA) was calculated, iii) Row0 TECs cold side heatsink (HS) temperature using the DS18B20 temperature sensors, with each TEC cold side heatsink fitted with a DS18B20 temperature sensor labeled T0 for TEC0, T1 for TEC1, T2 for TEC2 and T3 for TEC3 (and the same for T4 to T15 for TEC4 to TEC15 respectively when testing Row1 to Row3 TECs) as exemplified in Fig. 7, iv) Row0 TECs cold side heatsink cold maps using the Fluke Ti20 thermal imager and v) Row0 TECs input voltage, current and power. The TECs hot side water temperature was checked to be below 22 °C, if higher, it was replenished with cold water not <18 °C. This was to ensure that all the TECs measurements were reasonably conducted under similar performance test and environmental operational conditions with a ± 3 °C tolerance. The experiment was also repeated at 12 V for Row1 to Row3 TECs and then again at 10 V, 8 V, 6 V and 4 V for Row0 to Row 3 TECs. The 20 experiments results are presented next.

3. TECs measurements results

This section displays in what follows, the results summary of the 20 experiments execution methodology explained in Section 2.3. The ambient temperature of the test setup environment, the TECs hot side water temperature, the TECs cold side heatsink temperature, the TECs hot and cold sides temperature difference, the TECs cold side cold map, the TECs supply voltage, supply current and supply power were recorded.

3.1. Experiments 1 to 4 (TECs Row0 to Row3 at 12 V) results

The results of Experiments 1–4 were conducted at 12 V/5 A current limit as follows. Experiment 1 results of Row0 TECs (TEC0 to TEC3 with T0 to T3), Experiment 2 results of Row1 TECs (TEC4 to TEC7 with T4 to T7), Experiment 3 results of Row2 TECs (TEC8 to TEC11 with T8 to T11) and Experiment 4 results of Row3 TECs (TEC12 to TEC15 with T12 to T15). Note: the measurements were taken when the best performing TEC cooling stops/starts decreasing—this we termed the entropy point—- when the TEC Joule or Ohmic heating increases and causes the heat flow to stop or change direction as per the Second Law of Thermodynamics. The detailed raw measurements are found in the supplementary material Sections 3.1 to 3.4. The findings are summarised in Table 1.

3.2. Experiments 5 to 8 (TECs Row0 to Row3 at 10 V) results

The results of Experiments 5–8 were conducted at 10 V/5 A current limit as follows. Experiment 5 results of Row0 TECs (TEC0 to TEC3 with T0 to T3), Experiment 6 results of Row1 TECs (TEC4 to TEC7 with T4 to

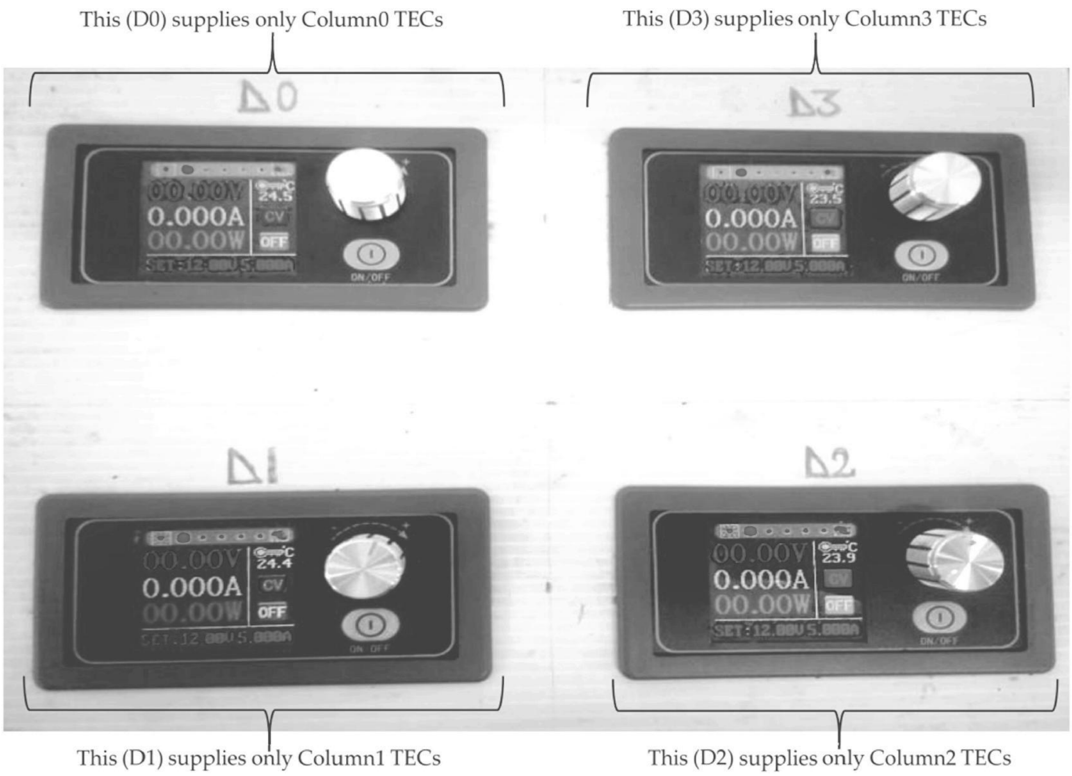

Fig. 8. Sinilink DC-DC power converters display.

Table 1
Experiments 1 to 4 (TEC0-3, TEC4-7, TEC8-11 and TEC12-15) at 12 V results summary.

All of these measurements were done at 12 V DC/5 A current limit and the lab ambient temperature was 19 °C

TECs	Cold-side HS Temp (°C) (DS18B20: T0-T15)		Hot-side H_2O Temp (°C) (MAX6675)				Temperature Difference (°C)	Voltage	Current	Power
TEC0-15			TH0	TH1	TH2	THA		(V)	(A)	(W)
TEC0	T0	4.19	20.75	21.00	21.00	20.92	16.73	12.00	2.685	32.22
TEC1	T1	−3.06	20.75	21.00	21.00	20.92	23.98	12.01	3.894	46.76
TEC2	T2	1.5	20.75	21.00	21.00	20.92	19.42	12.01	3.510	42.15
TEC3	T3	−6.12	20.75	21.00	21.00	20.92	27.04	12.00	3.945	47.34
TEC4	T4	8.06/7.87[a]	22.25	21.75	22.00	22.00	13.94/13.79[a]	12.00	3.634	43.60
TEC5	T5	0.75	22.25	21.75	22.00	22.00	21.25	12.00	3.296	39.55
TEC6	T6	−4.06	22.25	21.75	22.00	22.00	26.06	12.00	3.973	47.67
TEC7	T7	−0.37	22.25	21.75	22.00	22.00	22.37	12.00	3.958	47.49
TEC8	T8	2.12	23.5	22.5	24.75	23.58	21.46	12.01	3.552	42.65
TEC9	T9	12.63	23.5	22.5	24.75	23.58	10.96	12.01	3.791	45.52
TEC10	T10	−2.44	23.5	22.5	24.75	23.58	26.02	12.00	3.689	44.26
TEC11	T11	−1.56	23.5	22.5	24.75	23.58	25.15	12.00	3.854	46.24
TEC12	T12	7.31	21.00	21.00	21.5	21.17	13.85	12.00	3.307	39.68
TEC13	T13	2.5	21.00	21.00	21.5	21.17	18.67	12.01	3.494	41.96
TEC14	T14	−2.87	21.00	21.00	21.5	21.17	24.04	12.01	3.726	44.74
TEC15	T15	5.06	21.00	21.00	21.5	21.17	16.1	12.00	3.271	39.25

[a] This is the best reading noticed during that specific experiment but at a different instance to the measurements shown.

T7), Experiment 7 results of Row2 TECs (TEC8 to TEC11 with T8 to T11) and Experiment 8 results of Row3 TECs (TEC12 to TEC15 with T12 to T15). Note: the measurements were taken when the best performing TEC cooling stops/starts decreasing—this we termed the entropy point—-when the TEC Joule or Ohmic heating increases and causes the heat flow to stop or change direction as per the Second Law of Thermodynamics. The detailed raw measurements are found in the supplementary material Sections 3.5 to 3.8. The findings are summarised in Table 2.

3.3. *Experiments 9 to 12 (TECs Row0 to Row3 at 8 V) results*

The results of Experiments 9–12 were conducted at 8 V/5 A current limit as follows. Experiment 9 results of Row0 TECs (TEC0 to TEC3 with T0 to T3), Experiment 10 results of Row1 TECs (TEC4 to TEC7 with T4 to T7), Experiment 11 results of Row2 TECs (TEC8 to TEC11 with T8 to T11) and Experiment 12 results of Row3 TECs (TEC12 to TEC15 with T12 to T15). Note: the measurements were taken when the best performing TEC cooling stops/starts decreasing—this we termed the entropy point—when the TEC Joule or Ohmic heating increases and causes the heat flow to stop or change direction as per the Second Law of Thermodynamics. The detailed raw measurements are found in the supplementary material Sections 3.9 to 3.12. The findings are abridged in Table 3.

3.4. *Experiments 13 to 16 (TECs Row0 to Row3 at 6 V) results*

The results of Experiments 13–16 were conducted at 6 V/5 A current limit as follows. Experiment 13 results of Row0 TECs (TEC0 to TEC3 with T0 to T3), Experiment 14 results of Row1 TECs (TEC4 to TEC7 with T4 to T7), Experiment 15 results of Row2 TECs (TEC8 to TEC11 with T8 to T11) and Experiment 16 results of Row3 TECs (TEC12 to TEC15 with T12 to T15). Note: the measurements were taken when the best performing TEC cooling stops/starts decreasing—this we termed the entropy point—when the TEC Joule or Ohmic heating increases and causes the heat flow to stop or change direction as per the Second Law of Thermodynamics. The detailed raw measurements are found in the supplementary material Sections 3.13 to 3.16. The findings are summarised in Table 4.

Table 2
Experiments 5 to 8 (TEC0-3, TEC4-7, TEC8-11 and TEC12-15) at 10 V results summary.

All of these measurements were done at 10 V DC/5 A current limit and the lab ambient temperature was 19 °C

TECs	Cold-side HS Temp (°C) (DS18B20: T0-T15)		Hot-side H_2O Temp (°C) (MAX6675)				Temperature Difference (°C)	Voltage	Current	Power
TEC0-15			TH0	TH1	TH2	THA		(V)	(A)	(W)
TEC0	T0	5.06/4.94[a]	21.0	21.0	21.5	21.17	16.1/16.4[a]	10.00	2.111	21.11
TEC1	T1	−2.81	21.0	21.0	21.5	21.17	23.98	10.00	3.269	32.69
TEC2	T2	1.44	21.0	21.0	21.5	21.17	19.73	10.00	2.894	28.94
TEC3	T3	−5.5	21.0	21.0	21.5	21.17	26.67	10.01	3.308	33.11
TEC4	T4	5.19	19.75	19.75	20.00	19.83	14.65	10.01	3.089	30.92
TEC5	T5	−0.75	19.75	19.75	20.00	19.83	20.58	10.00	2.791	27.91
TEC6	T6	−5.44	19.75	19.75	20.00	19.83	25.27	10.00	3.372	33.72
TEC7	T7	−1.94	19.75	19.75	20.00	19.83	21.77	10.00	3.372	33.72
TEC8	T8	3	20.75	21.00	22.25	21.33	18.33	10.00	2.959	29.59
TEC9	T9	11.56	20.75	21.00	22.25	21.33	9.77	10.00	3.203	32.03
TEC10	T10	−0.69	20.75	21.00	22.25	21.33	22.02	10.00	3.057	30.57
TEC11	T11	0	20.75	21.00	22.25	21.33	21.33	10.00	3.248	32.48
TEC12	T12	4.06	20.75	19.25	19.75	19.92	15.85	10.01	2.857	28.59
TEC13	T13	−0.06	20.75	19.25	19.75	19.92	19.98	10.00	3.016	30.16
TEC14	T14	−4.25	20.75	19.25	19.75	19.92	24.17	10.00	3.180	31.80
TEC15	T15	2.75	20.75	19.25	19.75	19.92	17.17	09.99	2.768	27.65

[a] This is the best reading noticed during that specific experiment but at a different instance to the measurements shown.

Table 3
Experiments 9 to 12 (TEC0-3, TEC4-7, TEC8-11 and TEC12-15) at 8 V results summary.

All of these measurements were done at 8 V DC/5 A current limit and the lab ambient temperature was 18/19 °C										
TECs	Cold-side HS Temp (°C) (DS18B20: T0-T15)		Hot-side H_2O Temp (°C) (MAX6675)				Temperature Difference (°C)	Voltage	Current	Power
TEC0-15			TH0	TH1	TH2	THA		(V)	(A)	(W)
TEC0	T0	5.12/5.06[a]	19.5	19.75	20.25	19.83	14.71/15.1[a]	8.00	1.615	12.92
TEC1	T1	−2.75	19.5	19.75	20.25	19.83	22.58	8.00	2.619	20.95
TEC2	T2	1.25	19.5	19.75	20.25	19.83	18.58	8.00	2.260	18.08
TEC3	T3	−4.81	19.5	19.75	20.25	19.83	24.65	8.00	2.637	21.09
TEC4	T4	6.44	20.25	19.75	20.25	20.08	13.65	8.00	2.430	19.44
TEC5	T5	1.75	20.25	19.75	20.25	20.08	18.33	8.00	2.145	17.16
TEC6	T6	−3.00	20.25	19.75	20.25	20.08	23.08	8.00	2.674	21.39
TEC7	T7	0.13	20.25	19.75	20.25	20.08	19.96	8.03	2.682	21.53
TEC8	T8	1.94	20.5	20.75	21.75	21.00	19.06	8.00	2.400	19.20
TEC9	T9	8.63	20.5	20.75	21.75	21.00	12.38	8.00	2.561	20.48
TEC10	T10	−0.69	20.5	20.75	21.75	21.00	21.69	8.01	2.447	19.60
TEC11	T11	−0.44	20.5	20.75	21.75	21.00	21.44	8.00	2.607	20.85
TEC12	T12	3.06	18.25	17.75	18.00	18.00	14.94	8.00	2.254	18.03
TEC13	T13	−0.62	18.25	17.75	18.00	18.00	18.62	8.00	2.431	19.44
TEC14	T14	−3.19/−3.37[a]	18.25	17.75	18.00	18.00	21.19/21.37[a]	8.00	2.541	20.32
TEC15	T15	2.37	18.25	17.75	18.00	18.00	15.63	07.99	2.168	17.32

[a] This is the best reading noticed during that specific experiment but at a different instance to the measurements shown.

Table 4
Experiments 13 to 16 (TEC0-3, TEC4-7, TEC8-11 and TEC12-15) at 6 V results summary.

All of these measurements were done at 6 V DC/5 A current limit and the lab ambient temperature was 18 °C										
TECs	Cold-side HS Temp (°C) (DS18B20: T0-T15)		Hot-side H_2O Temp (°C) (MAX6675)				Temperature Difference (°C)	Voltage	Current	Power
TEC0-15			TH0	TH1	TH2	THA		(V)	(A)	(W)
TEC0	T0	7.62	18.00	18.25	18.75	18.33	10.71	06.01	1.144	06.87
TEC1	T1	0.19	18.00	18.25	18.75	18.33	18.15	06.00	1.937	11.62
TEC2	T2	4.06/4.00[a]	18.00	18.25	18.75	18.33	14.27/14.00[a]	06.00	1.608	09.64
TEC3	T3	−1.19	18.00	18.25	18.75	18.33	19.52	06.00	1.941	11.64
TEC4	T4	5.75/5.69[a]	18.25	18.00	18.75	18.33	12.58/12.65[a]	05.99	1.850	11.08
TEC5	T5	2.62	18.25	18.00	18.75	18.33	15.71	06.00	1.567	09.40
TEC6	T6	−1.94	18.25	18.00	18.75	18.33	20.27	05.99	2.001	11.98
TEC7	T7	0.81	18.25	18.00	18.75	18.33	17.52	06.00	2.005	12.03
TEC8	T8	3.87	18.75	18.25	19.00	18.67	14.79	06.00	1.769	10.61
TEC9	T9	9.56/9.5[a]	18.75	18.25	19.00	18.67	9.44/9.1[a]	06.00	1.827	10.96
TEC10	T10	1.75	18.75	18.25	19.00	18.67	16.92	06.01	1.795	10.78
TEC11	T11	1.81	18.75	18.25	19.00	18.67	16.85	06.00	1.942	11.65
TEC12	T12	4.94	18.5	18.5	18.75	18.58	13.65	06.00	1.614	09.68
TEC13	T13	1.69	18.5	18.5	18.75	18.58	16.9	05.99	1.795	10.75
TEC14	T14	−0.13	18.5	18.5	18.75	18.58	18.71	05.99	1.867	11.18
TEC15	T15	5.00	18.5	18.5	18.75	18.58	13.58	06.00	1.533	09.19

[a] This is the best reading noticed during that specific experiment but at a different instance to the measurements shown.

3.5. *Experiments 17 to 20 (TECs Row0 to Row3 at 4 V) results*

The results of Experiments 17–20 were conducted at 4 V/5 A current limit as follows. Experiment 17 results of Row0 TECs (TEC0 to TEC3 with T0 to T3), Experiment 18 results of Row1 TECs (TEC4 to TEC7 with T4 to T7), Experiment 19 results of Row2 TECs (TEC8 to TEC11 with T8 to T11) and Experiment 20 results of Row3 TECs (TEC12 to TEC15 with T12 to T15). Note: the measurements were taken when the best performing TEC cooling stops/starts decreasing—this we termed the entropy point—when the TEC Joule or Ohmic heating increases and causes the heat flow to stop or change direction as per the Second Law of Thermodynamics. The detailed raw measurements are found in the supplementary material Sections 3.17 to 3.20. The findings are summarised in Table 5.

Table 6 summarizes TEC0 - 15 cold side HS temperature measurements at 12 V, 10 V, 8 V, 6 V and 4 V, their $T_{cold\ mean}$, as well as their cooling rank (C_{rank}). Table 7 summarily categorizes TEC0 - TEC15 in terms of best, better, good and bad cooling performances.

Table 8 abridged the power consumed by TEC0 - TEC15 at 12 V, 10 V, 8 V, 6 V and 4 V including the mean input power ($P_{in\ mean}$), power consumption rank (P_{rank}) and C_{rank}. Table 9 ranked TEC0 to TEC15 in terms of their $P_{in\ mean}$ usage at 12 V, 10 V, 8 V, 6 V and 4 V. It simply shows the $P_{in\ mean}$ consumed and most importantly validates why TECs with low C_{rank} has high P_{rank}, but not necessarily vice versa. Also, least $P_{in\ mean}$ doesn't mean the best performance, since more power within limit, is required to produce more cooling.

Presented in Figs. 9–13 are Experiments 1 to 20 input power (Pin) versus the TECs (TEC0 - TEC15) cold side HS temperature (T_{cold}) performance summary, respectively at 12 V, 10 V, 8 V, 6 V and 4 V. Note the various performance dynamics.

Fig. 14 depicts the combined results of Experiments 1–20 represented in Figs. 9–13, now in a single plot to easily visualize how the TEC input power at 4 V, 6 V, 8 V, 10 V and 12 V, affects TEC0 - 15 cold side HS temperature and the cooling performance.

Now, what begs the in/efficiency question is, why are some of the TECs of the same made and model, especially TEC3, TEC6, TEC14 and TEC1 performed relatively best, whereas others such as TEC10, TEC7, TEC11 and TEC13 performed better, while TEC5, TEC2, TEC8 and

Table 5
Experiments 17 to 20 (TEC0-3, TEC4-7, TEC8-11 and TEC12-15) at 4 V results summary.

All of these measurements were done at 4 V DC/5 A current limit and the lab ambient temperature was 18 °C

TECs	Cold-side HS Temp (°C) (DS18B20: T0-T15)		Hot-side H_2O Temp (°C) (MAX6675)				Temperature Difference (°C)	Voltage	Current	Power
TEC0-15			TH0	TH1	TH2	THA		(V)	(A)	(W)
TEC0	T0	9.5	18.25	18.75	19.00	18.67	9.17	04.00	0.722	02.88
TEC1	T1	3.37	18.25	18.75	19.00	18.67	15.29	04.00	1.280	05.12
TEC2	T2	6.69	18.25	18.75	19.00	18.67	11.98	04.01	1.026	04.11
TEC3	T3	2.31	18.25	18.75	19.00	18.67	16.35	04.01	1.285	05.15
TEC4	T4	8.19/8.13[a]	18.5	18.5	18.75	18.58	10.4/10.21[a]	04.01	1.216	04.87
TEC5	T5	6.62	18.5	18.5	18.75	18.58	11.96	04.01	0.964	03.86
TEC6	T6	2.12	18.5	18.5	18.75	18.58	16.46	04.01	1.318	05.28
TEC7	T7	4.37/4.31[a]	18.5	18.5	18.75	18.58	4.21/14.27[a]	04.01	1.326	05.31
TEC8	T8	6.44/6.25[a]	18.75	18.25	19.5	18.83	12.4/12.58[a]	04.00	1.160	04.64
TEC9	T9	10.63	18.75	18.25	19.5	18.83	8.21	04.01	1.218	04.88
TEC10	T10	4.94	18.75	18.25	19.5	18.83	13.9	03.99	1.164	04.64
TEC11	T11	4.81	18.75	18.25	19.5	18.83	14.02	04.00	1.284	05.13
TEC12	T12	7.81	18.75	18.25	18.5	18.5	10.69	04.00	1.077	04.30
TEC13	T13	5.62	18.75	18.25	18.5	18.5	12.88	04.01	1.173	04.70
TEC14	T14	4.44/4.37[a]	18.75	18.25	18.5	18.5	14.06/14.21[a]	03.99	1.220	04.86
TEC15	T15	8.94	18.75	18.25	18.5	18.5	9.56	04.00	0.925	03.70

[a] This is the best reading noticed during that specific experiment but at a different instance to the measurements shown.

Table 6
Summary of TEC0 to TEC15 cold side HS temperature measurements at 12 V, 10 V, 8 V, 6 V and 4 V and Tcold mean.

TEC0 to TEC15 cold side HS temperature measurements at 12 V, 10 V, 8 V, 6 V and 4 V, as well as $T_{cold\ mean}$ (°C)

TECs	DS18B20	12 V	10 V	8 V	6 V	4 V	$T_{cold\ mean}$	C_{rank}
TEC0	T0 (°C)	4.19	5.06/4.94*	5.12/5.06*	7.62	9.5	6.262	14
TEC1	T1 (°C)	−3.06	−2.81	−2.75	0.19	3.37	−1.012	4
TEC2	T2 (°C)	1.5	1.44	1.25	4.06/4.00*	6.69	2.976	10
TEC3	T3 (°C)	−6.12	−5.5	−4.81	−1.19	2.31	−3.062	1
TEC4	T4 (°C)	8.06/7.87*	5.19	6.44	5.75/5.69*	8.19/8.13*	6.664	15
TEC5	T5 (°C)	0.75	−0.75	1.75	2.62	6.62	2.198	9
TEC6	T6 (°C)	−4.06	−5.44	−3.00	−1.94	2.12	−2.464	2
TEC7	T7 (°C)	−0.37	−1.94	0.13	0.81	4.37/4.31*	0.588	6
TEC8	T8 (°C)	2.12	3.00	1.94	3.87	6.44/6.25*	3.436	11
TEC9	T9 (°C)	12.63	11.56	8.63	9.56/9.5*	10.63	10.59	16
TEC10	T10 (°C)	−2.44	−0.69	−0.69	1.75	4.94	0.574	5
TEC11	T11 (°C)	−1.56	0	−0.44	1.81	4.81	0.924	7
TEC12	T12 (°C)	7.31	4.06	3.06	4.94	7.81	5.436	13
TEC13	T13 (°C)	2.5	−0.06	−0.62	1.69	5.62	1.826	8
TEC14	T14 (°C)	−2.87	−4.25	−3.19/−3.37*	−0.13	4.44/4.37*	−1.214	3
TEC15	T15 (°C)	5.06	2.75	2.37	5.00	8.94	4.824	12

*The best reading noted during that specific experiment but at a different instance to the measurements shown.

Table 7
Categorical summary of TEC0 to TEC15 cooling performance rank.

Remark	TEC0 to TEC15 ranking in terms of their mean cold side HS temperature ($T_{cold\ mean}$) in °C			
Best	TEC3 = $C_{rank}1$	TEC6 = $C_{rank}2$	TEC14 = $C_{rank}3$	TEC1 = $C_{rank}4$
	$T3_{cold\ mean}$ = −3.062	$T6_{cold\ mean}$ = −2.464	$T14_{cold\ mean}$ = −1.214	$T1_{cold\ mean}$ = −1.012
Better	TEC10 = $C_{rank}5$	TEC7 = $C_{rank}6$	TEC11 = $C_{rank}7$	TEC13 = $C_{rank}8$
	$T10_{cold\ mean}$ = 0.574	$T7_{cold\ mean}$ = 0.588	$T11_{cold\ mean}$ = 0.924	$T13_{cold\ mean}$ = 1.826
Good	TEC5 = $C_{rank}9$	TEC2 = $C_{rank}10$	TEC8 = $C_{rank}11$	TEC15 = $C_{rank}12$
	$T5_{cold\ mean}$ = 2.198	$T2_{cold\ mean}$ = 2.976	$T8_{cold\ mean}$ = 3.436	$T15_{cold\ mean}$ = 4.824
Bad	TEC12 = $C_{rank}13$	TEC0 = $C_{rank}14$	TEC4 = $C_{rank}15$	TEC9 = $C_{rank}16$
	$T12_{cold\ mean}$ = 5.436	$T0_{cold\ mean}$ = 6.262	$T4_{cold\ mean}$ = 6.664	$T9_{cold\ mean}$ = 10.59

TEC15 performed fairly good and finally TEC12, TEC0, TEC4 and TEC9 performed really bad—why the performance disparities—shouldn't they all perform fairly the same and like TEC3? Is TEC in/efficiency mostly just a misconception?

4. TECs measurements results interpretation

This section explains the TEC0 - TEC15 Experiments 1 to 20 results, summarily presented variously in Section 3—in tabular format in Tables 1–9 and in graphical format in Figs. 9–14, as well as the raw results in the supplementary material file. TEC0 - TEC15 Experiments 1 to 20 cold maps, cold side HS temperature, hot side water temperature and temperature difference readings, as well as the input voltage, current and power when TEC0-15 were operated at 12 V, 10 V, 8 V, 6 V and 4 V are interpreted.

4.1. Experiments 1 to 4 (TECs Row0 to Row3 at 12 V) results interpretation

TEC0 - TEC15 were powered firstly using 12 V and in groups of four per row and tested per row in turns as follows: Row0 consisting of TEC0-

Table 8
Summary of TEC0 to TEC15 input power measurements at 12 V, 10 V, 8 V, 6 V and 4 V, the $P_{in\ mean}$, P_{rank} and C_{rank}.

TECs	12 V P_{in} (W)	10 V P_{in} (W)	8 V P_{in} (W)	6 V P_{in} (W)	4 V P_{in} (W)	$P_{in\ mean}$ (W)	P_{rank}	C_{rank}
TEC0	32.22	21.11	12.92	06.87	02.88	15.200	1	14
TEC1	46.76	32.69	20.95	11.62	05.12	23.428	13	4
TEC2	42.15	28.94	18.08	09.64	04.11	20.584	5	10
TEC3	47.34	33.11	21.09	11.64	05.15	23.666	14	1
TEC4	43.60	30.92	19.44	11.08	04.87	21.982	9	15
TEC5	39.55	27.91	17.16	09.40	03.86	19.576	3	9
TEC6	47.67	33.72	21.39	11.98	05.28	24.008	15	2
TEC7	47.49	33.72	21.53	12.03	05.31	24.016	16	6
TEC8	42.65	29.59	19.20	10.61	04.64	21.338	6	11
TEC9	45.52	32.03	20.48	10.96	04.88	22.774	11	16
TEC10	44.26	30.57	19.60	10.78	04.64	21.970	8	5
TEC11	46.24	32.48	20.85	11.65	05.13	23.270	12	7
TEC12	39.68	28.59	18.03	09.68	04.30	20.056	4	13
TEC13	41.96	30.16	19.44	10.75	04.70	21.402	7	8
TEC14	44.74	31.80	20.32	11.18	04.86	22.580	10	3
TEC15	39.25	27.65	17.32	09.19	03.70	19.422	2	12

Table 9
Categorical summary of TEC0 to TEC15 mean input power consumption ranking.

Remark	TEC0 to TEC15 in terms of their mean input power ($P_{in\ mean}$) consumption in (W)			
Least	TEC0 = $P_{rank}1$	TEC15 = $P_{rank}2$	TEC5 = $P_{rank}3$	TEC12 = $P_{rank}4$
	$P_{in\ mean}$ = 15.200	$P_{in\ mean}$ = 19.422	$P_{in\ mean}$ = 19.576	$P_{in\ mean}$ = 20.056
Less	TEC2 = $P_{rank}5$	TEC8 = $P_{rank}6$	TEC13 = $P_{rank}7$	TEC10 = $P_{rank}8$
	$P_{in\ mean}$ = 20.584	$P_{in\ mean}$ = 21.338	$P_{in\ mean}$ = 21.402	$P_{in\ mean}$ = 21.970
More	TEC4 = $P_{rank}9$	TEC14 = $P_{rank}10$	TEC9 = $P_{rank}11$	TEC11 = $P_{rank}12$
	$P_{in\ mean}$ = 21.982	$P_{in\ mean}$ = 22.580	$P_{in\ mean}$ = 22.774	$P_{in\ mean}$ = 23.270
Most	TEC1 = $P_{rank}13$	TEC3 = $P_{rank}14$	TEC6 = $P_{rank}15$	TEC7 = $P_{rank}16$
	$P_{in\ mean}$ = 23.428	$P_{in\ mean}$ = 23.666	$P_{in\ mean}$ = 24.008	$P_{in\ mean}$ = 24.016

TEC3, Row1 constituting of TEC4-TEC7, Row2 comprising of TEC8-TEC11 and Row3 composing of TEC12-TEC15. In each experiment, the TECs input voltage, current, power, the TECs cold maps, the TECs cold and hot sides temperature, as well the temperature differences were recorded.

Experiment 1 raw results are displayed in Figure S1, in which TEC0-3 results are comparatively shown and analysed. As pictured in Figure S1a, TEC0-3 were all supplied using 12 V with 5 A current limit and then subjected to the same test conditions (19 °C lab ambient temperature and TECs hot side water average temperature of 20.92 °C as shown in Figure S1c highlighted in red). TEC3 drew the most current of 3.945 A/power of 47.34 W and consequently gave the best cooling of −6.12 °C as shown in Figure S1c highlighted in green, as well as evident in the cold map in Figure S1b—the darker blue the cold map is, the better the cooling. The next best cooling performance was given by TEC1, followed by TEC2 and finally TEC0—with its cold side HS temperature of 4.19 °C and input current of 2.685 A/power of 32.22 W. It's very interesting to see that all the TECs (TEC0-TEC3) performed differently (in/efficiently) under the same test conditions.

Experiment 2 raw results are displayed in Figure S2, in which TEC4-7 results are comparatively shown and analysed. As pictured in Figure S2a, TEC4-7 were all supplied using 12 V with 5 A current limit and then exposed to the same test conditions (19 °C lab ambient temperature and TECs hot side water average temperature of 22 °C as shown in Figure S2c highlighted in red). TEC6 slightly drew the most current of 3.973 A/power of 47.67 W and consequently gave the best cooling of −4.06 °C as shown in Figure S2c highlighted in green, as well as evident in the cold map in Figure S2b—the darker blue the cold map is, the better the cooling. The next best cooling performance was given by TEC7, followed by TEC5 and finally TEC4—with its cold side HS temperature of 7.87 °C and input current of 3.634 A/power of 43.6 W. It's very interesting to see that all the TECs (TEC4-7) also performed differently (in/efficiently) under the same test conditions.

Experiment 3 raw results are displayed in Figure S3, in which TEC8-11 results are comparatively shown and analysed. It's worth stating that Experiment 3 was repeated, as evident in the timestamp. This was because after Experiments 1 and 2, the TECs hot side water temperature got too high, up to about 30 °C (due to the high power and heat dissipation involved at 12 V), this affected Experiment 3 results; as a result, the TECs hot side temperature had to be first cooled <22 °C and the experiment redone. The TECs hot side water temperature still rose during operation but was kept below 25 °C (the highest in all the experiments) for Experiment 3 and the result was better. As pictured in Figure S3a, TEC8-11 were all supplied using 12 V with 5 A current limit and then subjected to the same test conditions (19 °C lab ambient temperature and TECs hot side water average temperature of 23.58 °C as shown in Figure S3c highlighted in red). TEC10 drew the third most current of 3.689 A/power of 44.26 W but interestingly gave the best cooling of −2.44 °C as shown in Figure S3c highlighted in green, as well as evident in the cold map in Figure S3b—the darker blue the cold map is, the better the cooling. The next best cooling performance of −1.56 °C was given by TEC11 (interestingly with the highest power usage of 46.24 W), followed by TEC8 and finally TEC9—with its cold side HS temperature of 12.63 °C and second highest input current of 3.791 A/power of 45.52 W. It's interesting to see that TECs (TEC8-11) have similar power dynamics but unlike the others, they performed more abnormally (in/efficiently) under the same test conditions.

Experiment 4 raw results are displayed in Figure S4, in which TEC12-15 results are comparatively shown and analysed. As pictured in Figure S4a, TEC12-15 were all supplied using 12 V with 5 A current limit and then subjected to the same test conditions (19 °C lab ambient temperature and TECs hot side water average temperature of 21.17 °C as shown in Figure S4c highlighted in red). TEC14 drew the most current of 3.726 A/power of 44.74 W and consequently gave the best cooling of −2.87 °C as shown in Figure S4c highlighted in green, as well as evident in the cold map in Figure S4b—the darker blue the cold map is, the better the cooling. The next best cooling result was given by TEC13, then by TEC15 and lastly TEC12—with its cold side HS temperature of 7.31 °C and third most input current of 3.307 A/power of 39.68 W. It's also interesting to see that under the same test conditions, all the TECs (TEC12-15) practically performed differently (in/efficiently), although almost proportionately as theoretically expected.

Experiments 1–4 results are summarised in Table 1 and Fig. 9. In

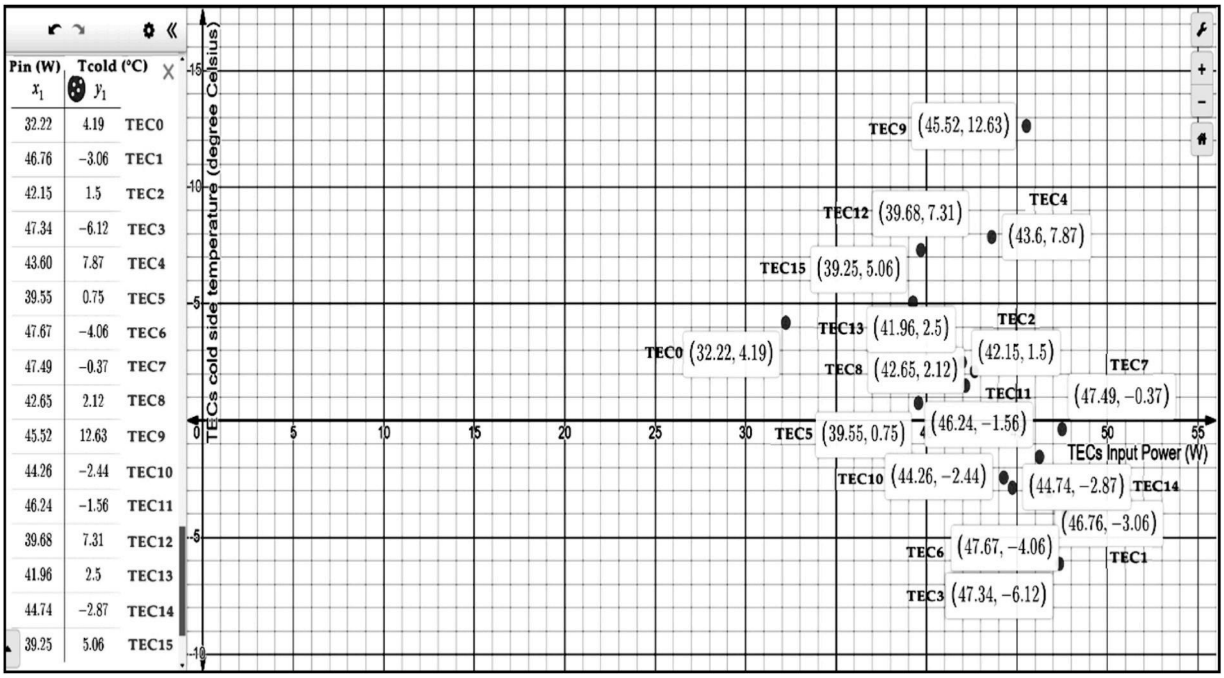

Fig. 9. Experiments 1–4 (TEC0-3, TEC4-7, TEC8-11 & TEC12-15) input power (W) vs TECs cold side HS temperature (°C) at 12 V.

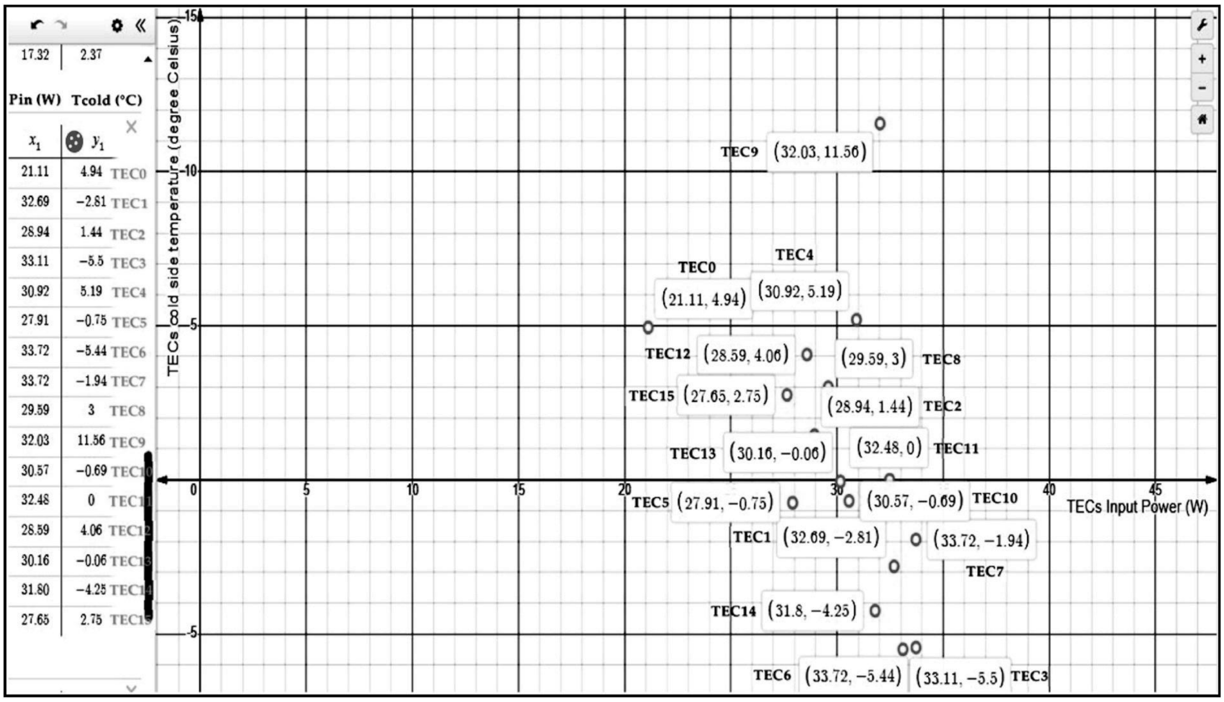

Fig. 10. Experiments 5–8 (TEC0-3, TEC4-7, TEC8-11 & TEC12-15) input power (W) vs TECs cold side HS temperature (°C) at 10 V.

sum, as apparent, TEC3 gave the best cooling performance, whereas TEC9 had the worst cooling performance. Of the 16 TECs tested at 12 V, the order of their best cooling performance (interestingly not entirely proportionate to the amount of input power/energy consumed) was as follows: TEC3, TEC6, TEC1, TEC14, TEC10, TEC11, TEC7, TEC5, TEC2, TEC8, TEC13, TEC0, TEC15, TEC12, TEC4 and TEC9—the first seven gave sub-zero cooling. As observed, the best cooling action is not necessarily directly proportional to the most power supplied. The cooling performance varied due to the TECs manufacturing quality, assembly and operational conditions. As clearly manifested in TEC10 and TEC11—both are of the same model and in same test conditions, but TEC10 gave better cooling results and at a lower power usage. Similarly with TEC6 and TEC3, though under slightly different test condition (both TECs hot sides temperature had a 1.08 °C THA difference), TEC6 consumed more power compared to TEC3, but gave lesser cooling. Of note also is how TEC9 had the 6th most input power relative to the rest, but had the worst cooling.

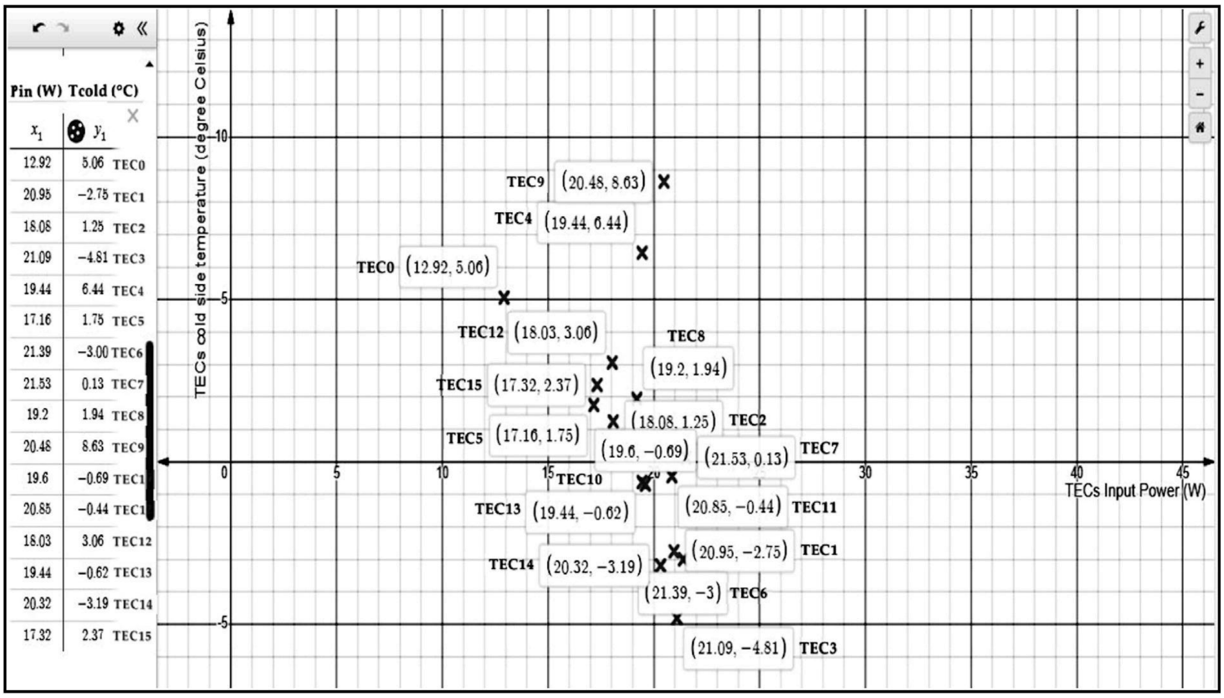

Fig. 11. Experiments 8–11 (TEC0-3, TEC4-7, TEC8-11 & TEC12-15) input power (W) vs TECs cold side HS temperature (°C) at 8 V.

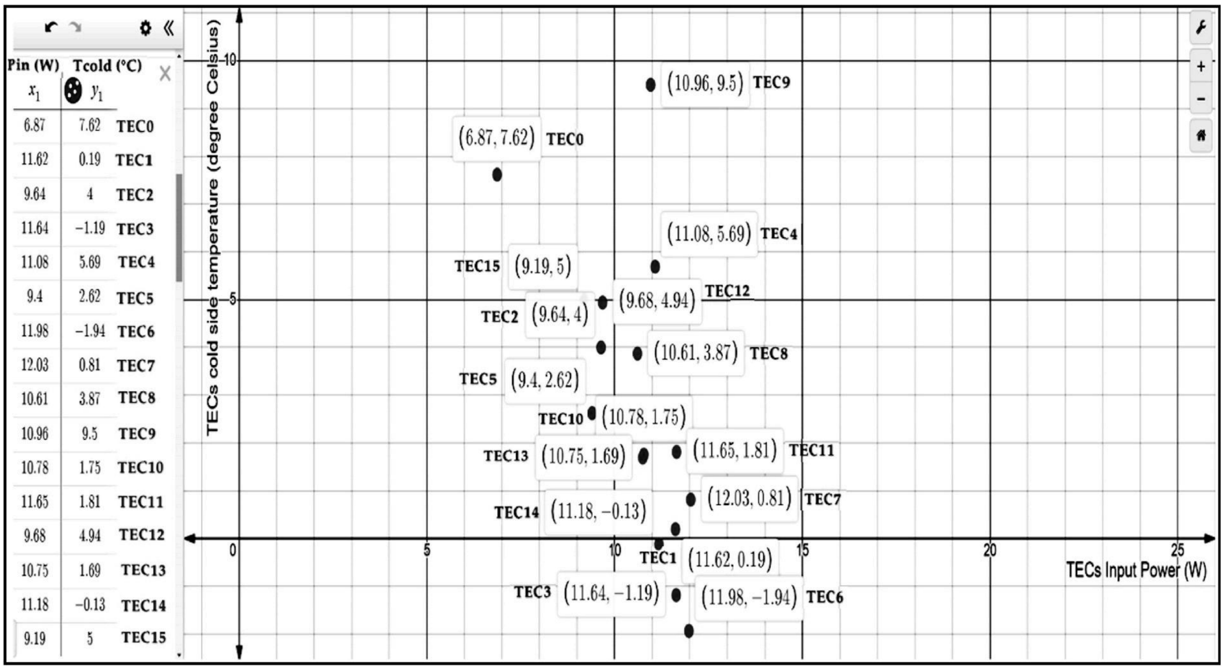

Fig. 12. Experiments 13–16 (TEC0-3, TEC4-7, TEC8-11 & TEC12-15) input power (W) vs TECs cold side HS temperature (°C) at 6 V.

4.2. Experiments 5 to 8 (TECs Row0 to Row3 at 10 V) results interpretation

TEC0 - TEC15 were powered now using 10 V and in groups of four per row and tested per row in turns as follows: Row0 consisting of TEC0-TEC3, Row1 constituting of TEC4-TEC7, Row2 comprising of TEC8-TEC11 and Row3 composing of TEC12-TEC15. In each experiment, the TECs input voltage, current, power, the TECs cold maps, the TECs cold and hot sides temperature, as well the temperature differences were recorded.

Experiment 5 raw results are displayed in Figure S5, in which TEC0-3 results are comparatively shown and analysed. As pictured in Figure S5a, TEC0-3 were all supplied using 10 V with 5 A current limit and then subjected to the same test conditions (19 °C lab ambient temperature and TECs hot side water average temperature of 21.17 °C as shown in Figure S5c highlighted in red). TEC3 drew the most current of 3.308 A/power of 33.11 W and consequently gave the best cooling of −5.5 °C as shown in Figure S5c highlighted in green, as well as evident in the cold map in Figure S5b—the darker blue the cold map is, the better the cooling. The next best cooling performance was given by

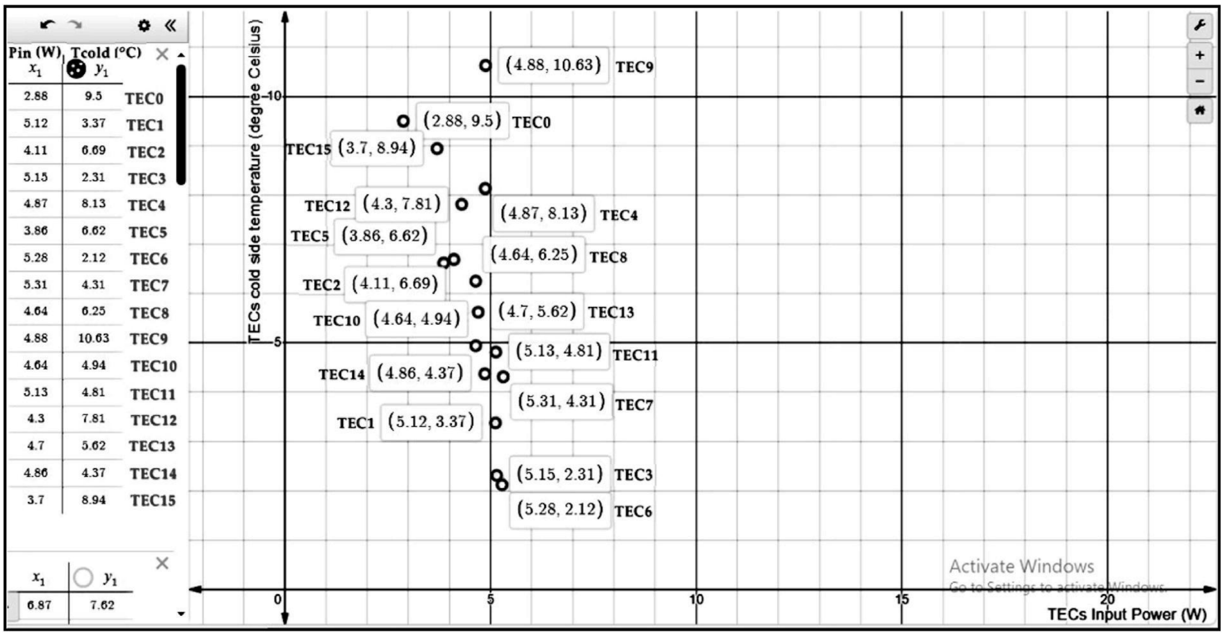

Fig. 13. Experiments 17–20 (TEC0-3, TEC4-7, TEC8-11 & TEC12-15) input power (W) vs TECs cold side HS temperature (°C) at 4 V.

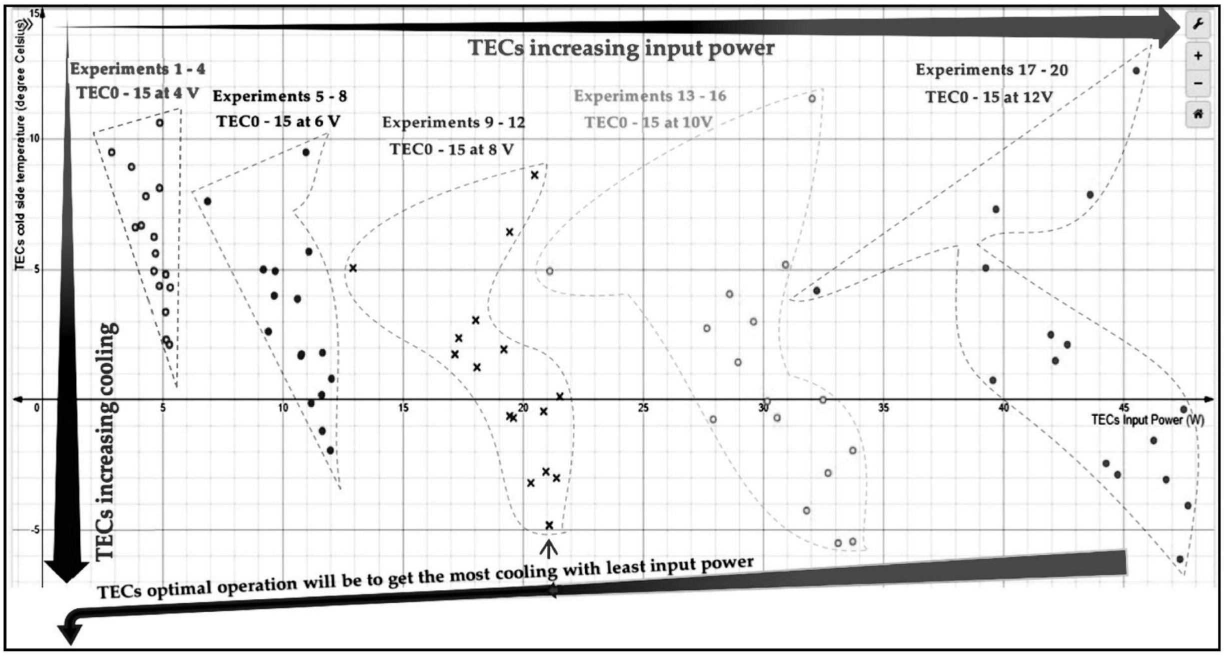

Fig. 14. Combined plot of Experiments 1 to 20 (TEC0 - TEC15) showing P_{in} (W) vs T_{cold} (°C) at 4 V, 6 V, 8 V, 10 V and 12 V.

TEC1, followed by TEC2 and finally TEC0—with its cold side HS temperature of 4.94 °C and input current of 2.111 A/power of 21.11 W. It's very interesting to see that all the TECs (TEC0-TEC3) performed differently (in/efficiently) under the same test conditions.

Experiment 6 raw results are displayed in Figure S6, in which TEC4-7 results are comparatively shown and analysed. As pictured in Figure S6a, TEC4-7 were all supplied with 10 V with 5 A current limit and then subjected to the same test conditions (19 °C lab ambient temperature and TECs hot side water average temperature of 19.83 °C as shown in Figure S6c highlighted in red). TEC6 and TEC7 drew the most and exactly the same current of 3.372 A/power of 33.72 W but TEC6 interestingly and consequently gave the best cooling of −5.4 °C as shown in Figure S6c highlighted in green, as well as evident in the cold map in Figure S6b—the darker blue the cold map is, the better the cooling. The next best cooling performance was given by TEC7, followed by TEC5 and finally TEC4—with its cold side HS temperature of 5.19 °C and input current of 3.089 A/power of 30.92 W. It's interesting to see that all the TECs (TEC4-7) also performed differently (in/efficiently) in the same test conditions, especially TEC6 and TEC7 with same power.

Experiment 7 raw results are displayed in Figure S7, in which TEC8-11 results are comparatively shown and analysed. As pictured in Figure S7a, TEC8-11 were all supplied using 10 V with 5 A current limit and then subjected to the same test conditions (19 °C lab ambient temperature and TECs hot side water average temperature of 21.33 °C as shown in Figure S7c highlighted in red). TEC10 drew the third most current of 3.057 A/power of 30.57 W but interestingly gave the best cooling of −0.69 °C as shown in Figure S7c highlighted in green, as well as evident in the cold map in Figure S7b—the darker blue the cold map is, the better the cooling. The next best cooling performance of 0 °C was given by TEC11 (interestingly with the highest power consumption of 32.48 W), followed by TEC8 and finally TEC9—with its cold side HS temperature of 11.56 °C and second highest input current of 3.203 A/power of 32.03 W. It's interesting to note that TECs (TEC8-11) have almost similar power dynamics/values, but unlike the other TECs results, they performed more abnormally (in/efficiently) under the same test conditions.

Experiment 8 raw results are displayed in Figure S8, in which TEC12-15 results are comparatively shown and analysed. As pictured in Figure S8a, TEC12-15 were all supplied using 10 V with 5 A current limit and then subjected to the same test conditions (19 °C lab ambient temperature and TECs hot side water average temperature of 19.92 °C as shown in Figure S8c highlighted in red). TEC14 drew the most current of 3.180 A/power of 31.80 W and consequently gave the best cooling of −4.25 °C as shown in Figure S8c highlighted in green, as well as evident in the cold map in Figure S8b—the darker blue the cold map is, the better the cooling. The next best cooling result was given by TEC13, then by TEC15 and finally TEC12—with its cold side HS temperature of 4.06 °C and third most input current of 2.857 A/power of 28.59 W. It's also interesting to see that under the same test conditions, all the TECs (TEC12-15) practically performed differently (in/efficiently), although almost proportionately as theoretically expected.

Experiments 5–8 results are abridged in Table 2 and Fig. 10. In sum, as obvious, TEC3 gave the best cooling performance, whereas TEC9 as usual, had the worst cooling performance. Of the 16 TECs tested at 10 V, the order of their best cooling performance (interestingly not entirely proportional to the amount of input power/energy consumed) was as follows: TEC3, TEC6, TEC14, TEC1, TEC7, TEC5, TEC10, TEC13, TEC11, TEC2, TEC15, TEC8, TEC12, TEC0, TEC4 and TEC9—the first eight gave sub-zero cooling. As observed, the best cooling action is not necessarily directly proportionate to the most power supplied. The cooling performance varied due to the TECs manufacturing quality, assembly and operational conditions. As clearly noted in TEC6 and TEC7—both are the same model, exact power consumption and under the same test conditions, but TEC6 gave far better cooling results. Similarly with TEC6 and TEC3, though under slightly different test condition (both TECs hot sides temperature had a 1.34 °C THA difference), TEC6 consumed more power compared to TEC3, but gave lesser cooling. Of note also is how TEC9 had the 6th most input power relative to the rest, but had the worst cooling.

4.3. Experiments 9 to 12 (TECs Row0 to Row3 at 8 V) results interpretation

TEC0 - TEC15 were powered now using 8 V and in groups of four per row and tested per row in turns as follows: Row0 consisting of TEC0-TEC3, Row1 constituting of TEC4-TEC7, Row2 comprising of TEC8-TEC11 and Row3 composing of TEC12-TEC15. In each experiment, the TECs input voltage, current, power, the TECs cold maps, the TECs cold and hot sides temperature, as well the temperature differences were recorded.

Experiment 9 raw results are displayed in Figure S9, in which TEC0-3 results are comparatively shown and analysed. As pictured in Figure S9a, TEC0-3 were all supplied using 8 V with 5 A current limit and then subjected to the same test conditions (18 °C lab ambient temperature and TECs hot side water average temperature of 18.83 °C as shown in Figure S9c highlighted in red). TEC3 drew the most current of 2.637 A/power of 21.09 W and accordingly gave the best cooling of −4.81 °C as depicted in Figure S9c highlighted in green, as well as evident in the cold map in Figure S9b—the darker blue the cold map is, the better the cooling. The next best cooling performance was given by TEC1, followed by TEC2 and finally TEC0—with its cold side HS temperature of 5.06 °C and input current of 1.615 A/power of 12.92 W. It's very interesting to see that all the TECs (TEC0-TEC3) performed differently (in/efficiently) under the same test conditions.

Experiment 10 raw results are displayed in Figure S10, in which TEC4-7 results are comparatively shown and analysed. As shown in Figure S10a, TEC4-7 were all powered using 8 V with 5 A current limit and then subjected to the same test conditions (19 °C lab ambient temperature and TECs hot side water average temperature of 20.08 °C as shown in Figure S10c highlighted in red). TEC7 slightly drew the most power and TEC6 drew a slightly 2nd highest current of 2.674 A/power of 21.39 W but interestingly gave the best cooling of −3.0 °C as shown in Figure S10c highlighted in green, as well as evident in the cold map in Figure S10b—the darker blue the cold map is, the better the cooling. The next best cooling performance was given by TEC7, then by TEC5 and lastly TEC4—with its cold side HS temperature of 6.44 °C and input current of 2.430 A/power of 19.44 W. It's very interesting to see that all the TECs (TEC4-7) also performed differently (in/efficiently) in the same test milieu—oddly TEC6 and TEC7 with almost same power.

Experiment 11 raw results are displayed in Figure S11, in which TEC8-11 results are comparatively shown and analysed. As portrayed in Figure S11a, TEC8-11 were all supplied using 8 V with 5 A current limit and then subjected to the same test conditions (19 °C lab ambient temperature and TECs hot side water average temperature of 21.0 °C as shown in Figure S11c highlighted in red). TEC10 drew the third most input current of 2.447A/power of 19.60 W but interestingly gave the best cooling of −0.69 °C as shown in Figure S11c highlighted in green, as well as evident in the cold map in Figure S11b—the darker blue the cold map is, the better the cooling. The next best cooling performance of −0.44 °C was given by TEC11 (interestingly with the highest power consumption of 20.85 W), then by TEC8 and lastly TEC9—with its cold side HS temperature of 8.63 °C and second highest input current of 2.561 A/power of 20.48 W. It's interesting to note that TECs (TEC8-11) have almost similar power values/dynamics, but unlike the other TECs results, they performed more abnormally (in/efficiently) under the same test conditions.

Experiment 12 raw results are displayed in Figure S12, in which TEC12-15 results are comparatively shown and analysed. As pictured in Figure S12a, TEC12-15 were all supplied using 8 V with 5 A current limit and then subjected to the same test conditions (18 °C lab ambient temperature and TECs hot side water average temperature of 18.0 °C as shown in Figure S12c highlighted in red). TEC14 drew the most current of 2.541 A/power of 20.32 W and consequently gave the best cooling of −3.37 °C as shown in Figure S12c highlighted in green, as well as evident in the cold map in Figure S12b—the darker blue the cold map is, the better the cooling. The next best cooling result was given by TEC13, followed by TEC15 and finally TEC12—with its cold side HS temperature of 3.06 °C and third most input current of 2.254 A/power of 18.03 W. It's also interesting to see that under the same test conditions, all the TECs (TEC12-15) practically performed differently (in/efficiently), although almost proportionately as theoretically expected.

Experiments 9–12 results are abridged in Table 3 and Fig. 11. In sum, as evident, TEC3 gave the best cooling performance, while TEC9 as expected had the worst cooling performance. Of the 16 TECs tested at 8 V, the order of their best cooling performance (interestingly not entirely proportional to the amount of input power/energy consumed) was as follows: TEC3, TEC14, TEC6, TEC1, TEC10, TEC13, TEC11, TEC7, TEC2, TEC5, TEC8, TEC15, TEC12, TEC0, TEC4 and TEC9—the first seven gave sub-zero cooling. As discovered, the best cooling action is not necessarily directly proportional to the most power supplied. The cooling performance varied due to the TECs manufacturing quality, assembly and operational conditions. As clearly noted in TEC6 and TEC7—both are the same model, almost the same power usage and in the same test conditions, but TEC6 gave far better cooling results. Similarly with TEC6 and TEC3, though under slightly different test condition (both TECs hot sides temperature had a 0.25 °C THA difference), TEC6 consumed more power relative to TEC3, but gave lesser cooling. Of note also is how TEC9 had the 6th most input power compared to the rest, but had the worst cooling.

4.4. Experiments 13 to 16 (TECs Row0 to Row3 at 6 V) results interpretation

TEC0 - TEC15 were supplied now with 6 V and in groups of four per row and tested per row in turns as follows: Row0 consisting of TEC0-TEC3, Row1 constituting of TEC4-TEC7, Row2 comprising of TEC8-TEC11 and Row3 composing of TEC12-TEC15. In each experiment, the TECs input voltage, current, power, the TECs cold maps, the TECs cold and hot sides temperature, as well the temperature differences were recorded.

Experiment 13 raw results are displayed in Figure S13, in which TEC0-3 results are comparatively shown and analysed. As shown in Figure S13a, TEC0-3 were all powered using 6 V with 5 A current limit and then subjected to the same test conditions (18 °C lab ambient temperature and TECs hot side water average temperature of 18.33 °C as shown in Figure S13c highlighted in red). TEC3 drew the most current of 1.941 A/power of 11.64 W and consequently gave the best cooling of −1.19 °C as depicted in Figure S13c highlighted in green, as well as evident in the cold map in Figure S13b—the darker blue the cold map is, the better the cooling. The next best cooling performance was given by TEC1, followed by TEC2 and finally TEC0—with its cold side HS temperature of 7.62 °C and input current of 1.144 A/power of 06.87 W. It's once more, keen to see that all the TECs (TEC0-TEC3) performed differently (in/efficiently) under the same test conditions.

Experiment 14 raw results are displayed in Figure S14, in which TEC4-7 results are comparatively shown and analysed. As shown in Figure S14a, TEC4-7 were all powered using 6 V with 5 A current limit and then subjected to the same test conditions (18 °C lab ambient temperature and TECs hot side water average temperature of 18.33 °C as shown in Figure S14c highlighted in red). TEC7 slightly drew the most power and TEC6 drew a slightly 2nd highest current of 2.001 A/power of 11.98 W but interestingly gave the best cooling of −1.94 °C as shown in Figure S14c highlighted in green, as well as evident in the cold map in Figure S14b—the darker blue the cold map is, the better the cooling. The next best cooling performance was given by TEC7, then by TEC5 and lastly TEC4—with its cold side HS temperature of 5.69 °C and input current of 1.85 A/power of 11.08 W. It's very interesting to see that all the TECs (TEC4-7) also performed differently (in/efficiently) in the same test milieu, oddly TEC6 and TEC7 with almost same power.

Experiment 15 raw results are displayed in Figure S15, in which TEC8-11 results are comparatively shown and analysed. As portrayed in Figure S15a, TEC8-11 were all supplied using 6 V with 5 A current limit and then subjected to the same test conditions (18 °C lab ambient temperature and TECs hot side water mean temperature of 18.67 °C as shown in Figure S15c highlighted in red). TEC10 drew the third most current of 1.795A/power of 10.78 W but interestingly gave the best cooling of 1.75 °C as shown in Figure S15c highlighted in green, as well as evident in the cold map in Figure S15b—the darker blue the cold map is, the better the cooling. The next best cooling performance of 1.81 °C was given by TEC11 (interestingly with the highest power consumption of 11.65 W), followed by TEC8 and lastly TEC9—with its cold side HS temperature of 9.5 °C and second highest input current of 1.827 A/power of 10.96 W. It's interesting to note that TECs (TEC8-11) have almost similar power values/dynamics, but unlike the other TECs results, they performed more abnormally (in/efficiently) under the same test conditions.

Experiment 16 raw results are displayed in Figure S16, in which TEC12-15 results are comparatively shown and analysed. As pictured in Figure S16a, TEC12-15 were all supplied using 6 V with 5 A current limit and then subjected to the same test conditions (18 °C lab ambient temperature and TECs hot side water mean temperature of 18.58 °C as shown in Figure S16c highlighted in red). TEC14 drew the most current of 1.867 A/power of 11.18 W and consequently gave the best cooling of −0.13 °C as shown in Figure S16c highlighted in green, as well as evident in the cold map in Figure S16b—the darker blue the cold map is, the better the cooling. The next best cooling result was given by TEC13, then by TEC12 and finally TEC15—with its cold side HS temperature of 5.0 °C and the least input current of 1.533 A/power of 09.19 W. It's also interesting to notice again that under the same test conditions, all the TECs (TEC12-15) practically performed differently (in/efficiently), although this time proportionately as theoretically expected.

Experiments 13–16 findings are abridged in Table 4 and Fig. 12. Interestingly, TEC6 gave the best cooling performance, while TEC9 as always, had the worst cooling performance. Of the 16 TECs tested at 6 V, the order of their best cooling performance (interestingly not entirely proportional to the amount of input power/energy consumed) was as follows: TEC6, TEC3, TEC14, TEC1, TEC7, TEC13, TEC10, TEC11, TEC5, TEC8, TEC2, TEC12, TEC15, TEC4, TEC0 and TEC9—the first three gave sub-zero cooling. As determined, the best cooling action is not necessarily directly proportional to the most supplied power. The cooling performance varied due to the TECs manufacturing quality, assembly and operational conditions. As clearly noted in TEC6 and TEC7—both are the same model, but TEC6 slightly drew lesser input power even though in the same test conditions and gave better cooling results. However, TEC6 and TEC3, though in exactly the same test condition (both TECs hot sides temperature had a 0 °C THA difference), TEC6 consumed more power relative to TEC3 and gave more cooling. Of note also is how TEC9 had the 8th most input power compared to the rest, but had the worst cooling.

4.5. Experiments 17 to 20 (TECs Row0 to Row3 at 4 V) results interpretation

TEC0 - TEC15 were supplied now with 4 V and in groups of four per row and tested per row in turns as follows: Row0 consisting of TEC0-TEC3, Row1 constituting of TEC4-TEC7, Row2 comprising of TEC8-TEC11 and Row3 composing of TEC12-TEC15. In each experiment, the TECs input voltage, current, power, the TECs cold maps, the TECs cold and hot sides temperature, as well the temperature differences were recorded.

Experiment 17 raw results are displayed in Figure S17, in which TEC0-3 results are comparatively shown and analysed. As shown in Figure S17a, TEC0-3 were all powered using 4 V with 5 A current limit and then subjected to the same test conditions (18 °C lab ambient temperature and TECs hot side water average temperature of 18.67 °C as shown in Figure S17c highlighted in red). TEC3 drew the most current of 1.285 A/power of 05.15 W and consequently gave the best cooling of 2.31 °C as depicted in Figure S17c highlighted in green, as well as evident in the cold map in Figure S17b—the darker blue the cold map is, the better the cooling. The next best cooling performance was given by TEC1, then by TEC2 and finally TEC0—with its cold side HS temperature of 9.5 °C and input current of 0.722 A/power of 02.88 W. It's once more interesting to see that all the TECs (TEC0-TEC3) performed differently (in/efficiently) under the same test conditions.

Experiment 18 raw results are displayed in Figure S18, in which TEC4-7 results are comparatively shown and analysed. As shown in Figure S18a, TEC4-7 were all powered using 4 V with 5 A current limit and then subjected to the same test conditions (18 °C lab ambient temperature and TECs hot side water average temperature of 18.58 °C as shown in Figure S18c highlighted in red). TEC7 slightly drew the most power and TEC6 drew a slightly 2nd highest current of 1.318 A/power of 05.28 W but interestingly gave the best cooling of 2.12 °C as shown in Figure S18c highlighted in green, as well as evident in the cold map in Figure S18b—the darker blue the cold map is, the better is the cooling. The next best cooling performance was given by TEC7, followed by TEC5 and finally TEC4—with its cold side HS temperature of 8.13 °C and input current of 1.216 A/power of 04.87 W. It's interesting to see that all the TECs (TEC4-7) also performed differently (in/efficiently) in the same test milieu, oddly TEC6 and TEC7 with almost same power.

Experiment 19 raw results are displayed in Figure S19, in which

TEC8-11 results are comparatively shown and analysed. As portrayed in Figure S19a, TEC8-11 were all supplied using 4 V with 5 A current limit and then subjected to the same test conditions (18 °C lab ambient temperature and TECs hot side water mean temperature of 18.83 °C as shown in Figure S19c highlighted in red). TEC11 drew the most current of 1.284/power of 05.13 W and consequently gave the best cooling of 4.81 °C as shown in Figure S19c highlighted in green, as well as evident in the cold map in Figure S19b—the darker blue the cold map is, the better the cooling. The next best cooling performance of 4.94 °C was given by TEC10 (with the 3rd/least highest power consumption of 04.64 W), followed by TEC8 and finally TEC9—with its cold side HS temperature of 10.63 °C and second highest input current of 1.218 A/ power of 04.88 W. It's interesting to note that TECs (TEC8-11) have almost similar power values/dynamics, but unlike the other TECs results, they performed more abnormally (in/efficiently) under the same test conditions.

Experiment 20 raw results are displayed in Figure S20, in which TEC12-15 results are comparatively shown and analysed. As pictured in Figure S20a, TEC12-15 were all supplied using 4 V with 5 A current limit and then subjected to the same test conditions (18 °C lab ambient temperature and TECs hot side water mean temperature of 18.50 °C as shown in Figure S20c highlighted in red). TEC14 drew the most current of 1.220 A/power of 04.86 W and consequently gave the best cooling of 4.37 °C as shown in Figure S20c highlighted in green, as well as evident in the cold map in Figure S20b—the darker blue the cold map is, the better the cooling. The next best cooling result was given by TEC13, then by TEC12 and finally TEC15—with its cold side HS temperature of 8.94 °C and the least input current of 0.925 A/power of 3.70 W. It's also interesting to notice again that under the same test conditions, all the TECs (TEC12-15) practically performed differently (in/efficiently), although this time proportionately as theoretically expected.

Experiments 17–20 findings are abridged in Table 5 and Fig. 13. Interestingly, TEC6 gave the best cooling performance, while TEC9 obviously had the worst cooling performance. Of the 16 TECs tested at 4 V, the order of their best cooling performance (interestingly not entirely proportional to the amount of input power/energy consumed) was as follows: TEC6, TEC3, TEC1, TEC7, TEC14, TEC11, TEC10, TEC13, TEC8, TEC5, TEC2, TEC12, TEC15, TEC4, TEC0 and TEC9—none of the TECs gave a sub-zero cooling. As found, the best cooling action is not necessarily directly proportional to the most power supplied. The cooling performance varied due to the TECs manufacturing quality, assembly and operational conditions. As clearly noted in TEC6 and TEC7—both are the same model, but TEC6 slightly drew lesser input power even though in the same test conditions and gave better cooling results. However, TEC6 and TEC3, though in exactly the same test condition (both TECs hot sides temperature had a 0.09 °C THA difference), TEC6 consumed more power relative to TEC3 and gave more cooling. Of note also is how TEC9 had the 6th most input power compared to the rest, but had the worst cooling.

5. Conclusion

Energy efficiency is primal to energy security, regardless of whether looking at it from a source and or load perspective. The more energy efficient an electrical load is, the less energy it consumes and the more energy can be saved and supply where it's needed. This manuscript practically examined the same TECs model with focus on the question of their energy in/efficiency. Sixteen TECs were used in the study and were tested in turns under similar conditions using 12 V, 10 V, 8 V, 6 V and 4 V with 5A current limit. Twenty experiments were conducted and the TECs cold side HS and hot side water temperatures, temperature difference, input voltage, current and power were captured variously and assorted inferences were made and represented/reported diversely. Based on TEC0 - TEC15 cold sides HS temperature and $T_{cold\ mean}$ at 12 V, 10 V, 8 V, 6 V and 4 V; the TECs results were tallied and abridged in Tables 6 and 8, while Table 7 employed $T_{cold\ mean}$ to categorical rank the TECs in terms of the best four, better four, good four and bad four. A TEC might initially (within 5–10 min) gives the best cooling but at a considerable higher input power (higher usage)—which over time, the constant high current drawn will, due to Joule heating and consequently entropy, negatively affect the cooling performance more quickly than when compared to a TEC of a slightly lesser cooling performance operated at a lower input power—which as a result, will give a longer and desirable cooling performance. TEC9 gave the worst result in terms of cooling (12.63 °C) and power consumption (45.52 W). TEC3 at 8 V gave the best optimal result in terms of cooling (−4.81 °C) and power consumption (21.09 W). Of interest also was TEC3 that gave the best cooling performance at 12 V, 10 V and 8 V but not at 6 V and 4 V—at which TEC6 cooling was best. In general, from Table 6 and Fig. 14 introspection, the best optimal result taking both cooling performance and power consumption into account was achieved at 8 V. In fact, at 8 V, six of the sixteen TECs; namely; TEC2, TEC8, TEC12, TEC13, TEC15 and even including TEC9 (the worst performed TEC), had their best cooling result ever, whereas the rest TECs performed relatively well considering their moderate power consumed. The reason why 8 V gave the TECs optimal result for the operational duration is because 8 V was enough to cause enough cooling but not enough to cause enough Ohmic heating. In light of this and based on the intended applications and available resources, trade-offs can always be made between faster cooling and less input power or energy consumption when using TECs. Now, imagine happening to buy, design and operate a TEC system with the likes of TEC9—what would be the misconceived conclusion—that TECs are very inefficient and impractical? In sum, it's clear designing with TECs is tricky, as sixteen TECs of the same type were used in the same test setup but all gave varying performances. While a TEC intrinsic chemistry is paramount for best performance, our findings further asserted that the TECs manufacturing/assembly quality, good design/implementation and sound operational physics knowledge by researchers/systems designers/users, are pivotal to get optimal performance from TECs. Future studies include TEDs as generators/heaters.

Funding

Cape Peninsula University of Technology's (CPUT) Research Directorate and the University of the Western Cape's (UWC) Hydrogen South Africa (HySA) Systems [R892].

CRediT authorship contribution statement

Nganyang Paul Bayendang: Conceptualization, Data curation, Formal analysis, Investigation, Methodology, Project administration, Resources, Software, Validation, Visualization, Writing – original draft, Writing – review & editing. **Vipin Balyan:** Formal analysis, Funding acquisition, Project administration, Resources, Supervision, Visualization, Writing – review & editing, Data curation. **Mohamed Tariq Kahn:** Data curation, Formal analysis, Funding acquisition, Project administration, Resources, Supervision, Validation, Writing – review & editing.

Declaration of competing interest

The authors declare the following financial interests/personal relationships which may be considered as potential competing interests: Authors declare financial and non-financial conflicts of interest with the funders.

Nganyang Paul Bayendang reports financial support was provided by University of the Western Cape. Vipin Balyan and Mohamed Tariq Kahn reports article publishing charges was provided by Cape Peninsula University of Technology. If there are other authors, they declare that they have no known competing financial interests or personal relationships that could have appeared to influence the work reported in this paper.

Data availability

Data will be made available on request.
Supplementary Material (Original data) ()

Acknowledgments

The authors are grateful to CPUT and UWC HySA Systems for the funding.

Appendix A. Supplementary data

Supplementary data to this article can be found online at https://doi.org/10.1016/j.rineng.2024.101827.

References

[1] United Nations, Sustainable Development Goals: Ensure Access to Affordable, Reliable, Sustainable and Modern Energy. https://www.un.org/sustainabledevelopment/energy/[Date Accessed: 9/September/2023].

[2] N.P. Bayendang, M.T. Kahn, V. Balyan, Combined cold, heat and power (CCHP) systems and fuel cells for CCHP applications: a topological review, Clean Energy 7 (Issue 2) (2023) 436–491, https://doi.org/10.1093/ce/zkac079.

[3] N.P. Bayendang, M.T. Kahn, V. Balyan, I. Draganov, S. Pasupathi, A Comprehensive Thermoelectric Cooler (TEC) Modelling, AIUE Congress, 2020, pp. 1–7, https://doi.org/10.2139/ssrn.3735378. International Conference on Use of Energy.

[4] A. Dąbrowska, M. Kobus, Ł. Starzak, B. Pękosławski, Analysis of efficiency of thermoelectric personal cooling system based on utility tests, Materials 15 (2022) 1115, https://doi.org/10.3390/ma15031115.

[5] A. Dąbrowska, M. Kobus, Ł. Starzak, B. Pękosławski, Evaluation of performance and power consumption of a thermoelectric module-based personal cooling system—a case study, Energies 16 (2023) 4699, https://doi.org/10.3390/en16124699.

[6] J. Gołębiowska, M.K. Widomski, Numerical assessment of the experimental thermoelectric cooling system effectiveness, Journal of Ecological Engineering 23 (12) (2022) 99–110, https://doi.org/10.12911/22998993/154845.

[7] A.E. Kabeel, M.G. Mousa, M.M.A. Elsayed, Theoretical study of thermoelectric cooling system performance, Journal of Engineering Research 3 (2019), https://doi.org/10.21608/erjeng.2019.125472.

[8] H. Dehra, Bringing Thermoelectricity into Reality: Building-Integrated Thermoelectric Cooling-Photovoltaic (TEC-PV) Devices, 2018, p. 386, https://doi.org/10.5772/intechopen.75472.

[9] A.C. Sulaiman, N.A.M. Amin, M.H. Basha, M.S.A. Majid, N.F.b.M. Nasir, I. Zaman, Cooling performance of thermoelectric cooling (TEC) and applications: a review, "MATEC Web Conf" 225 (2018) 10, https://doi.org/10.1051/matecconf/201822503021.

[10] P.I. Mani, Design, Modeling and Simulation of a Thermoelectric Cooling System (TEC), Western Michigan University, 2016. Masters Theses. 749, https://scholarworks.wmich.edu/masters_theses/749.

[11] C. Lundgaard, O. Sigmund, Design of segmented thermoelectric peltier coolers by topology optimization, Appl. Energy 239 (2019) 1003–1013, https://doi.org/10.1016/j.apenergy.2019.01.247.

[12] S. Manikandan, S.C. Kaushik, Energy and exergy analysis of an annular thermoelectric cooler, Energy Convers. Manag. 106 (2015) 804–814, https://doi.org/10.1016/j.enconman.2015.10.029.

[13] Z. Tark, A.J. Hamed, A.H.N. Khalifa, Performance study of the thermoelectric personal cooler under different ambient temperatures, International Journal of Heat and Technology 40 (1) (2022) 53–62, https://doi.org/10.18280/ijht.400107.

[14] Advanced Thermal Solutions. How to Select a Thermoelectric Cooler. https://www.qats.com/Download/Qpedia_May07_TEC_Selection4.ashx. [Date Accessed: 10/September/2023].

[15] F.L. Tan, S.C. Fok, Methodology on sizing and selecting thermoelectric cooler from different TEC manufacturers in cooling system design, Energy Convers. Manag. 49 (6) (2008) 1715–1723, https://doi.org/10.1016/j.enconman.2007.11.001.

[16] J. Patel, M. Patel, J. Patel, H. Modi, Improvement in the COP of thermoelectric cooler, International Journal of Scientific & Technology Research ume 5 (2016). Issue 05, https://www.ijstr.org/final-print/may2016/Improvement-In-The-Cop-Of-Thermoelectric-Cooler.pdf.

[17] H. Liu, G. Li, X. Zhao, X. Ma, C. Shen, Investigation of the impact of the thermoelectric geometry on the cooling performance and thermal—mechanic characteristics in a thermoelectric cooler, Energy 267 (2023), https://doi.org/10.1016/j.energy.2022.126471.

[18] T. Lu, X. Zhang, J. Zhang, P. Ning, Y. Li, P. Niu, Multi-objective optimization of thermoelectric cooler using genetic algorithms, AIP Adv. 9 (9) (2019) 095105, https://doi.org/10.1063/1.5119022.

[19] S. Lin, J. Yu, Optimization of a trapezoid-type two-stage peltier couples for thermoelectric cooling applications, Int. J. Refrig. 65 (2016) 103–110, https://doi.org/10.1016/j.ijrefrig.2015.12.007.

[20] T. Gong, Y. Wu, L. Gao, L. Zhang, J. Li, T. Ming, Thermo-mechanical analysis on a compact thermoelectric cooler, Energy 172 (2019) 1211–1224, https://doi.org/10.1016/j.energy.2019.02.014.

[21] R. Gouws, H. Eilers, A review on thermoelectric cooling modules: installation design, performance and efficiency, Sci. Res. Essays 8 (12) (2013) 485–492. https://academicjournals.org/article/article1380820851_Gouws%20and%20Eilers.pdf.

[22] Y.-W. Chang, C.-H. Cheng, W.-F. Wu, S.-L. Chen, An experimental investigation of thermoelectric air-cooling module, International Journal of Mechanical, Industrial and Aerospace Sciences 9 (2007), https://doi.org/10.5281/zenodo.1333628, 0.0.

[23] M. Siahmargoi, N. Rahbar, H. Kargarsharifabad, et al., An experimental study on the performance evaluation and thermodynamic modeling of a thermoelectric cooler combined with two heatsinks, Sci. Rep. 9 (2019) 20336, https://doi.org/10.1038/s41598-019-56672-9.

[24] J. Kaiprath, V.V. Kishor Kumar, A review on solar photovoltaic-powered thermoelectric coolers, performance enhancements, and recent advances, Int. J. Air-Cond. 31 (2023) 6, https://doi.org/10.1007/s44189-023-00022-y. Ref.

[25] N. Wang, et al., High efficiency thermoelectric temperature control system with improved proportional integral differential algorithm using energy feedback technique, in IEEE *Transactions on industrial electronics* 69 (5) (2022) 5225–5234, https://doi.org/10.1109/TIE.2021.3082462.

[26] Y. Lyu, et al., Experimental investigation of thermoelectric cooling for a new battery pack design in a copper holder, Results in Engineering 10 (2021) 100214, https://doi.org/10.1016/j.rineng.2021.100214.

[27] Z.R.A. Abdulghani, Novel experimental case study on optimization of peltier air cooler using Taguchi method, Results in Engineering 16 (2022) 100627, https://doi.org/10.1016/j.rineng.2022.100627.

[28] C. Lertsatitthanakorn, P. Bamroongkhan, J. Jamradloedluk, Performance study of thermoelectric dehumidification system integrated with heat pipe heatsink, Results in Engineering 17 (2023) 100901, https://doi.org/10.1016/j.rineng.2023.100901.

[29] G. Fabbri, M. Greppi, Numerical modeling of a new integrated PV-TE cooling system and support, Results in Engineering 11 (2021) 100240, https://doi.org/10.1016/j.rineng.2021.100240.

[30] Y. Tang, D. Jin, Z. Wang, F. Han, The extreme high cooling capacity thermoelectric cooler optimal design for kilowatts scale thermoelectric air-conditioner of high-speed railway carriage, Energy and Built Environment (2023), https://doi.org/10.1016/j.enbenv.2023.11.011.